Studies of Chiral Indoles. Part II*: Conformational Analysis of 1- and 3-(1-Phenylethyl) Indoles. A Dynamic ^{1}H NMR, Molecular Mechanics and Circular Dichroism Investigation

Ingemar Nilsson, Ulf Berg and Jan Sandström**

Division of Organic Chemistry 3, Chemical Center, University of Lund, P.O. Box 124, S-221 00 Lund, Sweden

Nilsson, I., Berg, U. and Sandström, J., 1986. Studies of Chiral Indoles. Part II: Conformational Analysis of 1- and 3-(1-Phenylethyl) Indoles. A Dynamic ^{1}H NMR, Molecular Mechanics and Circular Dichroism Investigation. – Acta Chem. Scand. B 40: 625–651.

The orientation of the 1-phenylethyl group in a series of 1- and 3-(1-phenylethyl)indoles was investigated by dynamic ^{1}H NMR and circular dichroism (CD) spectroscopy and by molecular mechanics calculation (MM2 force field). The 1-phenylethyl group was shown to adopt both a *syn* and an *anti* conformation, the equilibrium depending on the steric size of the substituent in position 2 (R^2). The study indicated similar *syn-anti* equilibria with the 1-phenylethyl group in 1 and 3 position when $R^2 = H$ or CH_3. However, when $R^2 = C(CH_3)_2OH$ or $-C(CH_3) = CH_2$, the 1-(1-phenylethyl)indoles showed strongly dominating *syn* conformations, while the temperature dependence of the CD spectra indicated that the 3- analogues had less biased *syn-anti* equilibria. ^{1}H DNMR showed that 1-methyl-2-isopropenyl-3-(1-phenylethyl)indole underwent hindered rotation of the isopropenyl group between two nearly equally populated sites, while the temperature-dependent CD spectrum indicated another more biased exchange, identified as the *syn-anti* exchange of the 1-phenylethyl group with a lower barrier and a dominant *syn* form. The rotational strengths obtained by theoretical calculations for the indole ^1L_b and ^1L_a transitions are in reasonably good agreement with those found experimentally.

Circular dichroism (CD) spectra are intrinsically very sensitive to the conformations of chiral molecules. Not only the magnitude but also the sign of a Cotton effect can change as the result of a conformatinal change. In spite of this sensitivity, the use of CD spectra in conformational analysis has been rather limited, partly due to the complexity of the theory for optical activity.

We have recently focused our attention on the possible utility of temperature-dependent CD in combination with dynamic NMR spectroscopy and molecular mechanics as a tool for conformational analysis. We have chosen to study chiral molecules consisting of a sp^3 hybridized atom with three different substituents, a chiral rotor attached to a planar framework. The indole ring was chosen as the planar framework mainly because the polarizations of its first $\pi \rightarrow \pi^*$ transitions are known from experiment.[1] In a previous work,[2] it was shown that an isopropyl group, when attached to an indole ring in either position 1 or 3, adopts one of two conformations, with the methine proton in or nearly in the sp^2 plane pointing either towards the benzene ring or towards the substituent in position 2. These conformations are similar to those adopted by the sugar residue in the purine nucleosides, wherefrom the well known *anti-syn* concept arises.[3]

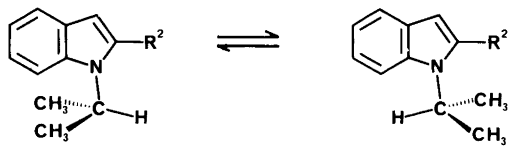

Syn *Anti*

*For Part I, see Ref. 5.

**To whom correspondence should be addressed.

The isopropyl group is replaced by a chiral rotor of the type CH_3CHX, where X is a chromophore. If the stable conformations are known and the chromophore X has well defined electrically and/or magnetically allowed transitions with known transition moments, it is possible to obtain the rotational strengths of the first $\pi \rightarrow \pi^*$ transitions in the indole ring from semiclassical calculations.[4]

The possibility of locating the chiral rotor in either position 1 or 3 allowed us to study the CD spectra in two systems with similar *syn-anti* equilibria but quite different spatial relations between the transition moments in the rotor and in the framework.[4] In this article, we present our results on conformational studies of 1-(1-phenylethyl)-2-R-indoles and 3-(1-phenylethyl)-2-R-indoles by dynamic ^1H NMR, CD spectroscopy and molecular mechanics calculations. The compounds included in this study and the anticipated *syn* and *anti* conformations are shown in Scheme 1.

Experimental

The preparation and enantiomer separation on microcrystalline triacetylcellulose of the chiral compounds included in this investigation, except for (*S*)-2,3-dimethyl-5-methoxy-1-(1-phenylethyl)-indole (*1g*), are described in Part I[5] of this series.

(*S*)-2,3-Dimethyl-5-methoxy-1-(1-phenylethyl) indole (*1g*) was obtained by treatment of *1f* with an excess of $LiAlH_4$ in dry ether at −40 °C for 1 h. After normal work-up,[6] flash chromatography[7] on silica gel (Merck 60, 230–400 mesh) in toluene/light petroleum (50:50) afforded *1g* in 50 % yield. Recrystallization from methanol/H_2O (95:5) gave pure crystals, m.p. 73.5–75.5 °C. MS [IP 70 eV; *m/z* (% rel. int.): 279 (M, 65), 175 (30), 160 (79), 105 (100). ^1H NMR (360 MHz, $(CD_3)_2O$, 25 °C): δ 1.86 (3H, d, *J* 7.2 Hz, CH_3CH), 2.20 (3H, s, 3-CH_3), 2.23 (3H, s, 2-CH_3), 3.74 (3H, s, 5-0-CH_3), 5.72 (1H, q, *J* 7.2 Hz, $CHCH_3$), 6.53 (1H, doublet of doublets, *J* 8.5, 2.2 Hz, *H*-6), 6.84 (1H, d, *J* 8.5 Hz, *H*-7), 6.88 (1*H*, d, *J* 2.2 Hz, *H*-4), 7.11–7.25 (5H, m).

The product obtained was not the expected one, since treatment of an ester with $LiAlH_4$ normally leads to a primary alcohol. However, in this case, a third hydride substitution took place in analogy with the reaction between arylalkyl ketones and $LiAlH_4/AlCl_3$.[8]

For ^1H NMR measurements, the variable temperature spectra of all compounds were recorded on a Nicolet Model 360 WB spectrometer with a variable temperature controller and internal deu-

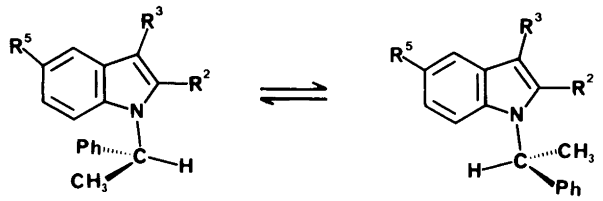

1a $R^2 = R^3 = R^5 = H$; *1b* $R^2 = CH_3$, $R^3 = R^5 = H$; *1c* $R^2 = COOMe$, $R^3 = R^5 = H$; *1d* $R^2 = C(CH_3)_2OH$, $R^3 = R^5 = H$; *1e* $R^2 = C(CH_3)=CH_2$, $R^3 = R^5 = H$; *1f* $R^2 = CH_3$, $R^3 = COOMe$, $R^5 = OMe$; *1g* $R^2 = R^3 = CH_3$, $R^5 = OMe$.

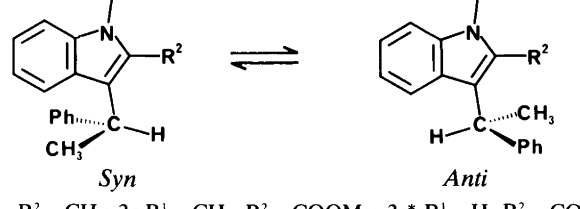

2a $R^1 = CH_3$, $R^2 = H$; *2b* $R^1 = R^2 = CH_3$; *2c* $R^1 = CH_3$, $R^2 = COOMe$; *2c** $R^1 = H$, $R^2 = COOMe$; *2d* $R^1 = CH_3$, $R^2 = C(CH_3)_2OH$; *2e* $R^1 = CH_3$, $R^2 = C(CH_3) = CH_2$.

Scheme 1.

terium lock, or, for *1f*, on a Jeol Model MH-100 spectrometer with standard variable temperature attachment. The samples were ca. 0.05 M in different solvent combinations, with dimethyl ether-d_6 as the main solvent providing the lock signal. Dichloromethane-d_2 and dichlorodifluoromethane (Freon 12) were the other solvents used in order to obtain solubility and a nonviscous solution at low temperatures. TMS was used as internal reference. The sample of *1f* was 0.5 M in dichlorofluoromethane with TMS added for the internal lock signal. All samples were degassed by the high vacuum freeze-thaw technique before being sealed off.[9] The temperature scale was calibrated by the use of a sample of methanol in dimethyl ether-d_6, which in turn, had been calibrated by the technique described in Ref. 10 using a Jeol MH-100 instrument. The fractional populations (p) and first order rate constants (k) were evaluated by visual fitting of the experimental spectra to theoretical spectra calculated by the McConnell formalism for uncoupled two-site exchange systems.[11,12] The evaluation of T_2 values for bandshape calculations was based on the bandwidths of reference signals unperturbed by exchange as previously described.[13] The free energies of activation and the free energy differences were calculated using eqn. (1) (based on the Eyring equation) and eqn. (2), were p_{syn} is the fractional population of the *syn* form. The cal-

$$\Delta G^{\ddagger}(syn \rightarrow anti) = RT \ln \frac{k_B \cdot T}{h \cdot k_{syn \rightarrow anti}} \qquad (1)$$

$$\Delta G^{\circ}(syn \rightarrow anti) = -RT \ln (p_{anti}/p_{syn}) \qquad (2)$$

culations were performed on a PDP 11/34 computer with a GT 42 graphics terminal and a Printronix lineprinter/plotter at the Computer Graphics Laboratory of the University of Lund. The chemical shifts for compounds *1–2* are shown in Table 1. N.O.e. difference experiments and 2-D homonuclear shift correlation experiments[14] were used to aid in the assignment of H-4, H-5, H-6 and H-7 of *1a, 2a* and *2b* in the room temperature spectra. These experiments were performed on a Varian XL-300. The p values, free activation energies and free energy differences for compounds *1b, 1f, 1g, 2c** and *2e* are found in Table 2.

The CD measurements were performed on a Jasco Model J41-A spectrometer. The cell for variable temperature measurements is described elsewhere.[15] The temperature of the sample was regulated by the boiling rate of the liquid nitrogen in a Dewar vessel, and monitored by a copper-constantan thermocouple dipping into the sample. The possibility of a temperature-dependent birefringence of the quartz windows was checked as proposed by Nordén,[16] and was found to be negligible. However, the isobestic points at wavelengths shorter than 240 nm were less clear for most of the compounds in this investigation. This may have been due to other contributing structures not seen at longer wavelength, but may also have been an artefact due to small distortions at lower temperature of the cell window in the thin cell (0.01 cm) used in this wavelength region. The samples were 0.8–3.2 mM in methanol. All CD measurements were run twice at room temperature, one with and one without the variable temperature equipment. No deviation could be observed if the baseline correction was run with the racemate of the same concentration instead of pure solvent. This was especially important when the absorption was strong compared to the rotational strength, even though the absorption was within the allowed limits for the instrument. Correction for the thermal contraction of methanol[17] was made for each spectrum relative to 293 K. The CD spectra shown in the figures are all corrected to 100 % ee.

The UV spectra were all recorded in methanol solution using Cary models 118 and 119 spectrophotometers.

The molecular mechanics calculations were performed using the program developed by Allinger *et al.* employing their 1977 force field (MM2),[18–20] excluding π electron calculations and with a rigid indole skeleton. The benzene ring was taken as a regular hexagon with 140 pm side, and the bond length and angles in the five-membered ring are shown in Fig. 1. Conformational energy maps for *1a, 1b, 2a* and *2b* were calculated as functions of the two dihedral angles θ_1 and θ_2 in steps of 10° from 0 to 360°. In *1a,b* θ_1 = C(2)-N(1)-C(10)-H(17) and θ_2 = N(1)-C(10)-C(11)-C(12); in *2a,b* θ_1 = C(2)-C(3)-C(10)-H(17) and θ_2 = C(3)-C(10)-C(11)-C(12) (Scheme 2). The calculations were performed by rotation around the specified bonds, all other geometric parameters being held fixed, *i.e.* stiff rotations. Only the torsional and electrostatic parameters

Table 1. ^{1}H Chemical shifts for compounds *1–2*.

Comp	Solvents	Temp /°C	CH_3CH	CH_3CH	R^1	R^2	*Syn/Anti* R^3	H-4	H-5	H-6	H-7
1a	$(CD_3)_2O/CCl_2F_2$	RT	1.88	5.68	–	7.29	6.46	7.50	6.99	6.94	7.16
	70:30	−141	1.88	5.68	–	7.72	6.53	7.52			
1b	$(CD_3)_2O$	RT	1.91	5.80	–	2.31	6.20	7.38	6.82–6.90		7.00
		−131	1.89/1.89	5.74/6.10	–	2.52/1.96	6.24/6.24	7.40/7.46			6.74/7.55
1c	$(CD_3)_2O$	RT	1.93	7.13		3.85	7.32	7.58		6.97–6.98[a]	
		−128	1.91	7.30		3.88	7.43	7.68	6.99, 7.04		6.92
1d	$(CD_3)_2O/CD_2Cl_2$	RT	1.95	6.78	–	1.67, 1.74	6.35	7.42	6.75, 6.85		6.75
	$/CCl_2F_2$ 60:20:20	−133	1.92	6.75		1.65, 1.73	6.42	7.47	6.75, 6.87		6.65
1e	$(CD_3)_2O/CCl_2F_2$	RT	1.89	5.90	–	2.17, 5.14, 5.34	6.41	7.46		6.80–6.92[a]	
	80:20	−135	1.87	6.03	–	2.23, 5.03, 5.39	6.58	7.47		6.82–6.92[a]	
1f	$CHCl_2F$	RT	1.94			2.76					
		−107	1.88/1.88			2.91/2.31					
1g	$(CD_3)_2O$	RT	1.86	5.72	–	2.23	2.20	6.88	3.73	6.53	6.84
		−124	1.85/1.85	5.66/5.94	–	2.42/1.89	2.26/2.16	6.88/6.95	3.70/3.77	6.37/6.71	6.58/7.35
2a	$(CD_3)_2O/CCl_2F_2$	RT	1.66	4.33	3.70	6.86	–	7.25	6.85, 7.05		7.21
	80:20	−135	1.61	4.27	3.76	7.20	–	7.30	6.82, 7.06		
2b	$(CD_3)_2O$	RT	1.75	4.45	3.60	2.30	–	7.33	6.99	6.83	7.19
		−140	1.74	4.44	3.63	2.44	–		6.99	6.81	
2c	$(CD_3)_2O/CCl_2F_2$	RT	1.78	5.25	3.86, 3.95		–	7.32	6.85, 7.18		7.32
	80:20	−135	1.77	5.26	3.93, 3.96		–	7.40	6.84, 7.14		7.14
								or 7.50			or 7.50
*2c**	$(CD_3)_2O$	RT	1.80	5.45	–	3.88	–	7.36	6.82, 7.12		7.30
		−131	1.78/1.78	5.65/5.34	–	3.92/3.92	–		6.88, 7.20		7.32/7.32
2d	$(CD_3)_2O/CD_2Cl_2$	RT	1.78	5.00	4.00	1.76, 1.78	–	7.09	6.72, 6.99		7.32
	$/CCl_2F_2$ 60:20:20	−140	1.76	4.93	4.07	1.82	–	6.98	6.68, 7.00		7.36
2e[b]	$(CD_3)_2O/CCl_2F_2$	RT	1.75	4.41	3.61	2.05, 5.10, 5.52	–	7.22	6.83, 7.03		7.30
	80:20	−143	1.72/1.76	4.33/4.33	3.65/3.65	2.19/2.11, 5.21/5.14, 5.65/5.59	–	7.22–7.30	6.78/6.83, 7.03/7.08		7.32–7.37

[a]H-5, H-6, H-7 are nearly overlapping. [b]Refers to the isopropenyl rotation.

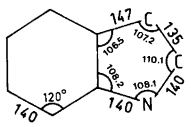

Fig. 1.

with respect to these two bonds and all van der Waals interactions were included in the calculations. The input geometry, except for the indole skeleton, was taken from ideal bond lengths, bond angles etc. included in the MM2 program. The construction of these idealized input geometries was facilitated by the molecular construction program MOLBUILD.[21] The minimum energy conformations obtained were then minimized using the full relaxation technique, except for the indole ring. New configurational maps were calculated as a function of θ_1 and θ_2, but the input geometries were taken as the mean values of the energy-minimized arrangements. The appearance of these maps did not significantly deviate from the original ones, but the energy minima were slightly more flattened. The reaction coordinate for the rotation of the 1-phenylethyl group was followed by constraining θ_1 in *1a,b* and *2a,b*, while allowing the energy to minimize with respect to other degrees of freedom. The forced rotation was performed in steps of 10° from 0–360°. MM calculations were also performed for *1e* and *2e*. The *syn* and *anti* minima were calculated with the isopropenyl group in the various possible energy minima. The *syn-anti* interconversion was also followed by constraining θ_1 and allowing relaxation of all other degrees of freedom. The conformational space for the reaction coordinate between the stable *syn* and *anti* structure was not fully explored and lower energy paths leading to the stable forms may exist. Finally, the reaction coordinate for the rotation of the isopropenyl group was followed by constraining the dihedral angle θ_3 = N(1)-C(2)-C(18)-C(19) for *1e* and θ_3 = C(3)-C(2)-C(18)-C(19) for *2e*, with the chiral rotor in the *syn* conformation (Scheme 3). The influence of the V_2 terms in the torsional parameters for the C(2)-C(18) bond was evaluated by calculating $\Delta E°$ and ΔE^* for the *syn-anti* exchange and for the isopropenyl group exchange while giving V_2 the values 7.5, 9.2 and 13 kJ mol^{-1}.

The limits of the utilized values for the V_2 term were estimated by making two MMP2 minimizations on 2-isopropenylindene, when the isopropenyl group is in the indene plane and perpendicular to the indene plane, respectively. The final V_2 terms 13 kJ mol^{-1} for the planar state and 7.5 kJ mol^{-1} for the perpendicular state were corrected for π electron effects. The parameters for the bond lengths and torsions within the phenyl ring of the chiral rotor were obtained by making a MMP2 calculation on toluene. The non standard force field parameters are shown in Table 3. The calculated energies and corresponding angles for the *syn-anti* exchange of *1a, 1b, 1e, 2a, 2b* and *2e* are found in Table 4, and the corresponding data for the isopropenyl group rotation of *1e* and *2e* are shown in Table 5.

The calculation of the rotational strengths of the electronic transitions was performed using the Schellman matrix formalism[22] in which all

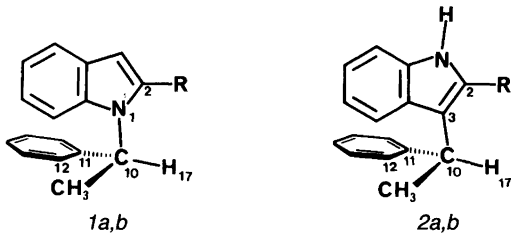

1a,b *2a,b*

Scheme 2.

Table 2. Fractional populations, ΔG^* and $\Delta G°$, determined by the DNMR technique.

Compound	Solvent	$p_{maj.}$	$\Delta G°_{(maj.\rightarrow min.)}$/kJ mol^{-1}	Temp/°C	$\Delta G^*_{(maj.\rightarrow min.)}$/kJ mol^{-1}	Temp/°C
1b	$(CD_3)_2O$	0.84	1.97	−131	36.5	−81
1f	$CHCl_2F$	0.94	3.75	−107	43.5	−73
1g	$(CD_3)_2O$	0.82	1.86	−124	37.0	−97
*2c**	$(CD_3)_2O$	0.75	1.30	−131	32.7	−113
2e	$(CD_3)_2O/CCl_2F$ 80:20	0.56	0.25	−143	33.3	−116

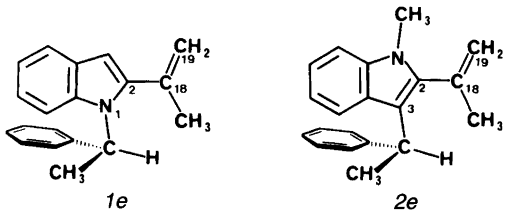

1e *2e*

Scheme 3.

three mechanisms that are considered to contribute to the rotational strength are incorporated. Since the four transitions of lowest energy in both the benzene and the indole chromophore are all $\pi \rightarrow \pi^*$ transitions, only the coupled oscillator mechanism[23,24] had to be considered for these compounds. The necessary input, except for the transition energies and dipole strengths for the benzene and indole chromophores in the distri-

Table 3. Force-field parameters (energies in kJ mol^{-1}).

Bond stretching	Bond type	l_o/Å	k_s/mdyn Å^{-1}
$E_s = 301.0\ k_s\ (l-l_o)^2[1 + C_s(l-l_o)]$	C(sp^3)-N(sp^2)	1.449	3.40
$C_s = -2.00$	C(sp^2)-C(sp^2)[a]	1.40	9.6
	C(sp^2)-C(sp^2)[b]	1.458	6.24
	C(sp^2)-C(sp^2)[b]	1.343	9.43
Bond bending	**Angle**	θ_o/deg	k_b/mdyn Å rad^{-2}
$E_b = 0.091688\ k_b\ (\theta-\theta_o)^2[1 + C_f(\theta-\theta_o)^4]$	C(sp^3)-N(sp^2)-C(sp^2)	121.0	0.70
$C_f = -0.006$	C(sp^3)-C(sp^2)-Nsp^2)	121.0	0.40
	C(sp^3)-C(sp^3)-N(sp^2)	109.47	0.42
	C(sp^2)-C(sp^3)-N(sp^2)	109.47	0.42
	H-C(sp^3)-N(sp^2)	109.47	0.42
	H-C(sp^2)-N(sp^2)	120.0	0.36

Torsion

$E_t = 0.5\ V_1\ (1 + \cos\omega) + 0.5\ V_2\ (1\text{-}\cos 2\ \omega) + 0.5\ V_3\ (1 + \cos 3\ \omega)$

Dihedral angle	V_1/kJ mol^{-1}	V_2/kJ mol^{-1}	V_3/kJ mol^{-1}
C(sp^3)-C(sp^2)-N(sp^2)-C(sp^2)	0	20.9	0
C(sp^3)-C(sp^2)-N(sp^2)-C(sp^3)	0	20.9	0
C(sp^3)-C(sp^3)-N(sp^2)-C(sp^2)	0	0	0
C(sp^2)-C(sp^3)-N(sp^2)-C(sp^2)	0	0	0
C(sp^2)-C(sp^2)-C(sp^3)-N(sp^2)	0	0	2.5
C(sp^2)-C(sp^2)-C(sp^2)-C(sp^2)[a]	−3.9	37.7	0
C(sp^3)-C(sp^2)-C(sp^2)-C(sp^2)[a]	−1.1	37.7	0
C(sp^2)-C(sp^2)-C(sp^2)-C(sp^2)[b]	−3.9	7.5, 9.2, 13.0	0
C(sp^2)-C(sp^2)-C(sp^2)-N(sp^2)[b]	−3.9	7.5, 9.2, 13.0	0
C(sp^3)-C(sp^2)-C(sp^2)-C(sp^2)[b]	−1.1	7.5, 9.2, 13.0	0
C(sp^3)-C(sp^2)-C(sp^2)-N(sp^2)[b]	−1.1	7.5, 9.2, 13.0	0
H-C(sp^3)-N(sp^2)-C(sp^2)	0	0	4.2
H-C(sp^2)-N(sp^2)-C(sp^3)	0	25.1	0
H-C(sp^2)-N(sp^2)-C(sp^2)	0	25.1	0
H-C(sp^2)-C(sp^2)-C(sp^2)[a]	0	37.7	−4.4
H-C(sp^2)-C(sp^2)-C(sp^3)[a]	0	37.7	0
H-C(sp^2)-C(sp^2)-H[a]	0	37.7	0

[a]Parameters for the phenyl ring obtained from a MMP2 calculation for toluene.
[b]Parameters for the indole-isopropenyl group obtained by MMP2 calculations for 2-isopropenylindene.

Table 4. Calculated conformational energies and barriers to *syn-anti* interconversion for *1a, 1b, 2a, 2b, 1e* and *2e*[a] as a function of the dihedral angles θ_1, θ_2 and θ_3.[b]

Comp	V_2/kJ mol^{-1}	Minimum energy conformation θ_1°	θ_2°	θ_3°	Energy/kJ mol^{-1} conformation	Lowest transition state θ_1°	θ_2°	θ_3°	Energy barrier *syn*→*anti*/kJ mol^{-1}
1a	–	−7.5	+58.0	– (*syn*)	0.38	−60	+76	–	15.2
		−126.0	+132.0	– (*anti 1*)	0				
		+163.2	+64.6	– (*anti 2*)	0.80				
1b	–	−11.6	+54.1	– (*syn*)	0	−70	+97	–	26.7
		+161.1	+56.6	– (*anti*)	2.18				
		−172.3	+59.9	– (local *anti*)[c]	7.0				
2a	–	−11.3	+60.1	– (*syn*)	2.34	−60	+77	–	9.3
		−125.6	+126.5	– (*anti 1*)	0				
		+166.6	+69.8	– (*anti 2*)	3.06				
2b	–	−16.2	+57.5	– (*syn*)	0	−70	+97	–	17.1
		+163.4	+56.3	– (*anti*)	0.63				
		−170.7	+63.6	– (local *anti*)[c]	3.26				
1e	9.2	−6.0	+55.0	+142.7 (*syn 1*)	0	−69	+84	−140	24.2
		−6.3	+54.4	−42.1 (*syn 2*)	0.63				
		−5.8	+44.8	−140.1 (*syn 3*)	2.7				
		−4.5	+45.0	+46.0 (*syn 4*)	3.6				
		+145.0	−125.1	+56.2 (*anti 1*)	4.3				
		+150.6	−130.0	−119.4 (*anti 2*)	7.0				
		−171.2	−138.9	+131.8 (*anti 3*)	7.2				
		−170.2	−137.2	−59.3 (*anti 4*)	8.9				
	7.5	−5.6	+55.2	+136.7 (*syn 1*)	0	−69	+83	−136	20.9
		−5.9	+54.4	−46.7 (*syn 2*)	0.5				
		+143.6	−125.0	+59.8 (*anti 1*)	2.6				
	13.0	−6.4	+55.0	+152.6 (*syn 1*)	0	−69	+84	−145	26.7
		−7.1	+54.7	−34.4 (*syn 2*)	1.0				
		+143.6	−132.7	+39.9 (*anti 1*)	6.4				
2e	9.2	−4.6	+62.4	−54.5 (*syn 1*)	0	−70	+92	+56	15.8
		−3.7	+61.2	+127.0 (*syn 2*)	0.13				
		+145.4	+61.6	+63.6 (*anti 1*)	1.4				
		+148.9	+59.1	−111.4 (*anti 2*)	4.2				
	7.5	−4.4	+62.4	−57.8 (*syn 1*)	0	−70	+91	+60	15.5
		−3.6	+61.5	+123.4 (*syn 2*)	0.13				
		+145.6	+61.2	+65.0 (*anti 1*)	0.64				
	13.0	−5.2	+61.0	−47.2 (*syn 1*)	0.12	+110	+74	+63	21.8
		−6.7	+61.0	+134.9 (*syn 2*)	0				
		+142.0	+56.0	+53.3 (*anti 1*)	3.0				

[a]The calculations have been performed for the *S* configuration. [b]See text for the definition of θ_1, θ_2 and θ_3. [c]Not discovered during forced rotation.

buted monopole approximation, was obtained from CNDO/S-CI calculations in the version of Guimon *et al.*,[25] using configurational interactions among the 99 most low-lying configurations.

A summary of the results of the molecular orbital calculations for indole is presented in Table 6. The calculated transition moment polarizations for the indole ^1L_b and ^1L_a transitions are in reasonably good agreement with the experimental results[1] (Table 6). However, in the final calculations of the rotational strengths the calculated transition moment directions and set of transition monopoles were adjusted to fit the ex-

perimental transition moment by solving a constrained minimization problem with Lagrange multipliers as proposed by Rizzo and Schellman.[26] No experimental determination of the polarizations of the indole ^1B_b and ^1B_a transitions has been reported. Other directions for the ^1B_b transition than our CNDO/S values have been obtained by PPP calculations by Goux *et al.*[27] and for the ^1B_a transition by Yamamoto and Tanaka,[1] but the former calculation failed to predict the correct sign of $\boldsymbol{R}$ for the ^1B_b transition of yohimbic acid. Using the Lagrange multiplier technique, a number of sets of transition monopoles was calculated for the ^1B_b and ^1B_a transitions, covering the directions reported by the other workers, starting from the original CNDO/S values. These data were used as input in trial calculations aimed at finding polarizations of the ^1B_b and ^1B_a transitions which could reproduce the experimental CD bands. The calculations were performed for the *S* configuration for both the 1- and 3-(1-phenylethyl)indoles.

The experimental oscillator strengths and transition energies for the ^1L_a, ^1L_b and ^1B_b transitions were taken from the work of Yamamoto and Tanaka[1] (Table 6), while the oscillator strength for ^1B_a was arbitrarily chosen as slightly less than that of ^1B_b. Strickland and Billups[28] reported slightly different oscillator strengths for the indole ^1L_b and ^1L_a transitions, but in view of the uncertainties of the other input data, we regard these differences as of minor importance. The midpoints of the moments of the transitions in the indole chromophore were placed in the center of the C(8)-C(9) bond (see figure in Table 7). The corresponding transition monopoles, shown in Table 7, were scaled to reproduce the experimental and estimated transition moments and were placed for simplicity in the centra of the atoms.

The transition moments for the benzene chromophore were calculated from toluene spectra using the expression $\mu^2 = 9.18 \cdot 10^{-3} \int(\varepsilon/\lambda)d\lambda$. The data for the ^1L_b and ^1L_a transitions were taken from experimental spectra, and those for the absorption band at 188 nm from the vacuum UV spectrum by Shorygin *et al.*[29] We ascribed this band to the ^1B_a transition (parallel to the C(11)-C(14) bond) and the ^1B_b (perpendicular to this bond, see figure in Table 7)[30,31] and we assumed the two transitions have equal strength. The transition monopoles for all four transitions were taken from the CNDO/S calculation using the aforementioned technique (Table 7).

Maps of the rotational strengths ($\boldsymbol{R}$) for the four indole and four benzene transitions were calculated by the Schellman method, varying θ_1 from 0 to 360° and θ_2 from 0 to 180°, both in steps of 10°. By superposing these maps over those obtained by the MM calculations, $\boldsymbol{R}$ values for re-

Table 5. Calculated conformational energies and barriers to the 2-isopropenyl group rotation for *1e* and *2e* as a function of the dihedral angle θ_3°,[a] with the chiral rotor in the *syn* region.

Compound	V_2/kJ mol^{-1}	Minimum energy conformation θ_3°	Energy/kJ mol^{-1}	Lowest transition state conformation θ_3°	Energy/kJ mol^{-1}
1e	9.2	−42.1	0.63	180	12.8
		−140.1	2.7		
		+142.7	0		
		+46.0	3.6		
	13.0	−34.4	0.67	10	14.8
		−152.2	2.9		
		+152.6	0		
		+36.5	4.2		
2e	9.2	−54.5	0	180	35.6
		+127.0	0.13		
	13.0	−47.2	0.13	180	25.3
		+134.9	0		

[a]See text for the definition of θ_3.

Table 6. CNDO/S calculations for the singlet states of indole.

Transition	Energy[a] /eV	Oscillator strength[a]	Polarization direction[a] (α)
^1L_b	4.32 (4.4)	0.0035 (0.010)	+44.4° (54°)
^1L_a	4.26 (4.6)	0.0174 (0.112)	−42.2° (−38°)
^1B_b	5.73 (5.8)	0.180 (0.680)	+5.8°
^1B_a	6.08 (6.2)	0.0993	−39.1°

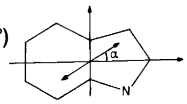

[a]The values in parentheses are experimental values from Ref. 1.

gions around the energy minima are readily obtained. Values for the minima are found in Table 8.

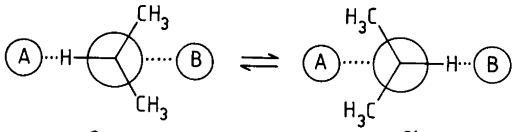

3a *3b*

Results and discussion

It has been shown that isopropyl groups attached to a planar framework adopt one of two bisected conformations,[10,32-34] *3a* and *3b*, and that the position of the equilibrium is governed by the relative sizes of the flanking entities, i.e. the form *3a* is favoured when $A > B$ and *vice versa*. In 1-isopropylindoles,[2] with H-7 and R^2 as the flanking entities, no exchange effects on the ^{1}H NMR spectra were observed when $R^2 = H$ and $R^2 = C(CH_3)_2OH$. In the latter case, this is probably due to a strong dominance of the *syn* rotamer, while in the former, it may either be due to a strong preponderance of the *anti* rotamer, a low barrier, or both. When $R^2 =$ Me or CO_2Me, *syn-anti* equilibria were observed with the *syn* form as the dominating conformation, and with free energy barriers of 46.2 and 44.7 kJ mol^{-1}, respectively. The 3-isopropyl analogues, with H-4

Table 7. Transition monopoles.

Atom		Charges in atomic units for the indicated transitions			
		^1L_b (+54°)	^1L_a (−38°)	^1B_b (+5.8°)	^1B_a (−39.1°)
Indole	N(1)	0.10666	−0.00470	0.19724	−0.43534
	C(2)	−0.09258	0.32902	0.51638	0.33812
	C(3)	0.04378	−0.26204	−0.48178	−0.14276
	C(4)	0.04280	−0.51496	0.32128	0.19284
	C(5)	−0.02462	0.48336	−0.27344	0.12628
	C(6)	0.01568	−0.52346	0.08574	0.07064
	C(7)	0.05142	0.50764	−0.37000	0.07910
	C(8)	−0.06462	−0.49508	−0.10718	−0.24144
	C(9)	−0.07850	0.48175	0.10944	0.01254
		^1L_b (0°)	^1L_a (90°)	^1B_b (0°)	^1B_a (90°)
Toluene	C(11)	0.0	−0.13844	0.0	−0.22900
	C(12,16)	±0.03060[a]	−0.06184	±0.20608[a]	±0.10280
	C(13,15)	±0.00876[a]	0.08428	±0.17188[a]	0.13942
	C(14)	0.0	0.10228	0.0	0.16918

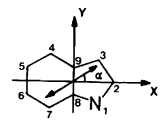

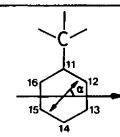

[a]The same sign for C(12) and C(13).

Table 8. Calculated rotational strengths for compounds *1a, 1b, 2a* and *2b.*[a]

Compound	Conformation	***R*** (D×BM)							
		Indole				Benzene			
		^1L_b	^1L_a	^1B_b	^1B_a	^1L_b	^1L_a	^1B_b	^1B_a
1a	*syn*	−0.033	+0.060	+0.4	−0.5	−0.037	−0.75	+1.8	−1.0
	anti 1	+0.035	−0.020[b]	−0.8	+0.48	+0.032	+0.85	−1.7	+1.1
	anti 2	+0.014	−0.060[b]	−3.5	−0.48	−0.006[b]	+0.37	+0.8	+1.9
1b	syn	−0.033	+0.060	+0.30	−0.48	−0.038	−0.70	+1.8	−1.0
	anti	+0.019	−0.060	−3.2	−0.35	−0.001[b]	+0.57	+0.30	+2.0
	local *anti*	+0.018	−0.070	−4.3	−0.54	−0.01[b]	+0.34	+1.4	+2.4
2a	*syn*	−0.064	−0.40	−1.0	−2.2	+0.012	+1.2	+3.1	−0.70
	anti 1	+0.0069	+0.41	+1.4	+2.1	−0.009	−1.2	−3.1	+0.60
	anti 2	+0.0008[b]	−0.03[b]	+0.3	+0.2[b]	+0.010	−0.70	+0.2[b]	−0.10[b]
2b	*syn*	−0.0061	−0.40	−0.80	−2.2	+0.013	+1.2	+3.0	−0.70
	anti	−0.0010[b]	+0.07[b]	+0.5	+0.80[b]	+0.006[b]	−0.70	−1.1[b]	−0.10
	local *anti*	+0.0006[b]	−0.03[b]	+0.8	−1.0[b]	+0.017	−1.0	+1.3[b]	0.0

[a]*S* configuration. [b]Close to nodal line.

and R^2 as flanking entities, probably exhibit a similar behaviour, but due to low barriers (<35 kJ mol^{-1}) and unfavourable rotamer distributions, they are less amenable to NMR studies.

With this background, we present below experimental and theoretical results which indicate that compounds *1a–e* and *2a–e* exhibit similar *syn-anti* equilibria. We also demonstrate the changes in the CD spectrum. which are the consequences of conformational changes, and the possibility of revealing dynamic equilibria, not accessible by the NMR technique, by measuring the rotational strengths as functions of the temperature. Finally, we present theoretical calculations of the rotational strengths based on the Schellman matrix formalism,[22] to ascertain whether the theoretical model is capable of reproducing, at least qualitatively, the experimental rotational strength and thereby giving valuable conformational information.

Table 9. Ultraviolet spectra of compounds *1a–g* and *2a–e.*[a]

Compound	λ_{max}/nm (ε)	λ_{max}/nm (ε)	λ_{max}/nm (ε)	λ_{max}/nm (ε)	λ_{max}/nm (ε)
1a	291.5 (5400)	281.0 (6900)	274.0 (6800)	264 (sh, 6500)	219.0 (37600)
1b	290.5 (6400)	280.0 (8000)	274.5 (7700)	269.5 (sh, 7300)	221.5 (35100)
1c	308.0 (sh, 10500)	293.5 (18900)	228.0 (21100)	204.5 (30300)	
1d	292.0 (6800)	282.5 (8700)	275.0 (8400)	269.0 (sh, 8000)	222.0 (36600)
1e	291.5 (10900)	287.0 (sh, 10500)	221.0 (sh, 24000)	215.0 (25700)	205.0 (27800)
1f	303.5 (sh, 9700)	293.5 (sh, 14300)	286.5 (14800)	242.5 (22500)	217.0 (42300)
1g	309.0 (sh, 5200)	303.0 (sh, 6600)	298.0 (7300)	284.5 (8400)	228.5 (25800)
2a	296.5 (sh, 5400)	290.0 (6100)	279.0 (sh, 5400)	272.0 (sh, 4900)	225.0 (36400)
2b	293.5 (6700)	286.0 (7000)	280.0 (sh, 6200)	273.5 (sh, 5500)	228.5 (34400)
2c	311.0 (sh, 12000)	296.0 (21200)	230.0 (29300)	206.0 (28000)	
*2c**	310.0 (sh, 12500)	296.0 (20500)	230.0 (29000)	203.5 (31500)	
2d	296.5 (sh, 6000)	290.0 (6800)	280.0 (sh, 6300)	270.0 (5100)	227.0 (30000)
2e	291.2 (8300)	227.5 (30400)			

[a]All spectra have been recorded in methanol solution.

Table 10. CD spectra of compounds *1a–g* and *2a–e*. $\lambda_{extremes}$, nm ($\Delta\varepsilon$).[a]

Compound	Temp/°C	λ/nm ($\Delta\varepsilon$)			
1a	+22	293.0 (−2.5)	286.5 (−2.2)	274.0 (sh, −0.9)	235.5 (sh, +12.7)
		224.5 (+28.2)	206 (−9.9)	201 (neg.min., −9.1)	
	−95	293.0 (−3.9)	286.0 (−3.7)	271.0 (−1.9)	235.0 (sh, +17.4)
		225.5 (+34.7)	206.0 (−15.1)	201.5 (neg.min., −11.8)	
1b	+22	291.5 (−1.4)	285.5 (−0.7)	270.0 (sh, +0.7)	265 (sh, +1.1)
		227.0 (sh, +9.8)	221.5 (+13.7)	210.0 (−12.4)	202 (neg.min., −10.0)
	−96	291.5 (−2.9)	284.5 (−1.6)	281.5 (sh, −0.5)	270.5 (sh, +1.1)
		263.5 (sh, +1.7)	228 (sh, +17.3)	222.0 (+22.1)	210.5 (−22.1)
1c	+22	325.0 (+2.5)	314.0 (+2.7)	285 (−2.4)	257.5 (+1.5)
		240.0 (−7.4)	221.0 (−9.8)	206.5 (+10.5)	
	−81	327.5 (+3.2)	314.0 (+3.6)	285.0 (−2.7)	256.0 (+2.7)
		241.0 (−12.1)	220.0 (−16.1)	205.0 (+14.5)	
1d	+21	294.0 (−4.3)	286.5 (−2.5)	270.0 (+1.4)	265.0 (+2.0)
		224.0 (+36.3)	207.0 (−22.3)	202.0 (neg.min., −20.7)	
	−90	294.5 (−6.3)	287.0 (−3.1)	270.0 (+1.5)	265.0 (+2.0)
		223.0 (+38.8)	210.5 (−28.8)	201.5 (neg.min., −22.8)	
1e	+21	322.5 (+0.1)	293.5 (−1.8)	246.5 (+6.8)	237.5 (pos.min., +6.0)
		222.5 (+19.4)	210.0 (−9.8)		
	−92	325.0 (+0.1)	294.5 (−2.5)	269.0 (sh, +2.4)	250.5 (+10.0)
		239.0 (pos.min., +5.3)	222.0 (+18.3)	210.0 (−11.6)	
1f	+22	302.5 (sh, −1.4)	297.0 (−1.5)	266.5 (−0.7)	259.0 (−0.7)
		234.0 (sh, +6.0)	222.5 (+14.3)	209.0 (−14.2)	201.5 (neg.min., −8.2)
	−95	306.0 (sh, −2.5)	297.0 (−2.9)	265.0 (−2.0)	259.0 (−2.4)
		254.5 (−2.1)	235.0 (sh, +8.6)	221.0 (+24.3)	210.0 (−21.4)
1g	+23	314.0 (−0.9)	308.5 (−0.9)	304.0 (−0.8)	270.0 (sh, +1.1)
		266.0 (+1.2)	259.0 (+1.2)	231.0 (+6.4)	207.5 (−10.2)
	−95	314.0 (−2.0)	307.5 (−1.4)	302.0 (−1.4)	271.5 (+2.0)
		265.0 (+2.1)	231.0 (+8.1)	225.0 (sh, +6.8)	210.0 (−15.7)
2a	+22	300.0 (−2.4)	293.0 (−2.6)	276.0 (−2.4)	268.5 (−1.5)
		231.0 (+12.4)	222.5 (sh, +6.2)	207.5 (pos.min., +0.4)	198.5 (+11.5)
	−88	301.5 (−3.9)	294.0 (−4.2)	277.5 (−3.6)	271.5 (−3.8)
		266.5 (−2.8)	261.0 (sh, −0.9)	229.0 (+15.8)	222.0 (sh, +8.7)
		208.5 (−1.3)	197.5 (+13.8)		
2b	+22	297.5 (−2.0)	291.0 (−2.0)	280.0 (−1.8)	240.0 (sh, +5.1)
		224.0 (+12.4)	207.0 (−2.50)		
	−87	297.5 (−3.4)	291.0 (−3.5)	281.0 (−3.1)	272.5 (−3.1)
		267.5 (−2.0)	241.5 (sh, 4.3)	229.5 (+20.2)	207.5 (pos.min., +0.8)
2c	+21	322.0 (+4.5)	297.5 (+6.0)	271.0 (+2.5)	264.0 (+1.3)
		257.0 (−0.3)	251.5 (+0.3)	235.0 (−20.0)	221.0 (−16.8)
		203.0 (+2.4)	194.0 (+26.4)		
	−92	321.0 (+6.2)	296.5 (+8.3)	293.0 (+7.6)	270.0 (+3.8)
		264.0 (+2.1)	255.5 (−0.2)	250.5 (+1.1)	234.5 (−29.1)
		221.0 (−21.2)	203.0 (+7.1)	192.0 (+50.3)	
*2c**	+20	317.5 (sh, +4.7)	295.0 (+8.9)	270.5 (+3.8)	263.5 (sh, +2.0)
		253.5 (−0.7)	249.0 (+0.3)	232.0 (−29.8)	225.0 (sh, −24.9)
	−95	326.5 (+6.1)	293.5 (+10.6)	270.0 (+5.2)	263.5 (+2.6)
		254.0 (−1.5)	247.5 (+1.6)	232.0 (−40.7)	220.0 (−28.1)
2d	+22	302.0 (−4.3)	293.5 (−4.3)	279.0 (−4.1)	259.5 (sh, −0.8)
		224.0 (+19.7)	208.5 (−4.0)	201.0 (+4.7)	
	−92	303.5 (−5.8)	294.0 (−5.9)	279.0 (−5.4)	223.0 (+23.0)
		207.0 (−8.4)	200.0 (neg.min., −0.9)		
2e	+23	298.0 (−2.8)	284.0 (sh, −2.5)	271.0 (−2.0)	266 (sh, −1.3)
		226.0 (sh, +14.2)	223.0 (+15.2)	208.0 (−0.3)	199.5 (+6.3)
	−92	301.0 (−4.4)	288.0 (sh, −3.7)	271.0 (−3.3)	265.0 (−2.1)
		230.0 (+19.1)	224.0 (+18.9)	209.0 (−1.0)	200.0 (+3.5)

[a]All spectra have been recorded in methanol solution.

^{1}H NMR results and molecular mechanics calculations. In the ^{1}H NMR spectrum of *1b*, the resonances of two forms were observed in the ratio of 84:16 at −131 °C. The assignment of the minor rotamer to the *anti* conformation is based on the observation that the ^{1}H resonance of the rotor methine (H_α) appeared at δ 6.10 in the minor and at δ 5.74 in the major rotamer. This can be attributed to the strong deshielding by the benzene part of the indole ring, in the minor form, observed also for the isopropyl analogue. The force field calculations for *1b* are in excellent agreement with the experimental result (Table 4). According to the calculations, *1b* has two energy minima (Fig. 2). The *syn* form is calculated to be of 2.18 kJ mol^{-1} lower energy than the *anti* form, very close to the experimental value, 1.97 kJ mol^{-1}. In both forms, the phenyl ring, which approaches the flanking entities face on, is closer to the flanking groups than the methyl group in the rotor. This is in agreement with the upfield shift of the ^{1}H resonance of the 2-methyl group [δ(2-Me)] of the *anti* rotamer and of H-7 of the *syn* rotamer, respectively, due to the shielding effect of the phenyl ring in the rotor. This also indicates that the effective size of the phenyl ring, which varies considerably[35] with the direction of approach, in this system appears slightly smaller than that of a methyl group. The calculated barrier is 9.7 kJ mol^{-1} lower than that found experimentally, a deviation also found for the isopropyl analogue.

In *1f* and *1g syn-anti* equilibria similar to those in *1b* are observed in the ^{1}H NMR spectra at low temperature; the free energy difference obtained for *1g* is almost the same as for *1b* (Table 2), in close resemblance to that of the isopropyl analogues,[2] while the equilibrium of *1f* is more biased. This is due to the buttressing of the methyl group exerted by the 3-methoxycarbonyl group which also results in a higher barrier to *syn-anti* interconversion in *1f*.

No exchange effects were observed on the ^{1}H resonances of *2b* from ambient temperature down to −136 °C. The δ(2-Me) value is, however, shifted from 2.31 to 2.44 ppm. With the reasonable assumption that the δ(2-Me) is similar in the *syn* forms of *1b* and *2b* as well as in their *anti* forms, the displacement indicates a similar *syn-anti* equilibrium for *2b* as for *1b*. Support for the assumption of the similarity of the shift of the *syn* form is obtained from the 1- and 3-isopropyl analogues, δ(2-Me) being 2.30–2.36 in the *syn* forms, and 2.32 (unresolved) in the 3-derivative. Furthermore, the calculated conformational map of *2b* is almost identical to that of *1b*. On the other hand, $\delta(H_\alpha)$ for *2b* is almost temperature-independent, which indicates a strongly biased equilibrium, assuming similar shift differences as for *1b*. The differences in $\delta(H_\alpha)$ between the *syn* and *anti* forms may, however, be smaller in *2b* than in *1b*, as has been generally observed for indoles with other chiral rotors in position 1 and 3.[36] Assuming a similar difference in the barriers between *1b* and *2b* as is found between the 1- and 3-isopropyl groups of 1,3-diisopropyl-2-methylindole,[2] a barrier of 23 kJ mol^{-1} is estimated for the *syn-anti* exchange in *2b*. Assuming a shift difference not larger than for the 2-Me group of *1b*, $\Delta G^\circ_{(syn\text{-}anti)}$ *ca.* 2 kJ mol^{-1} as for *1b* and a natural bandwidth of *ca.* 4 Hz, the temperature at which the intensity of the 2-Me resonance in *2b* should be diminished to 50 % by exchange broadening was calculated as −157 °C. Thus, a low barrier and not a strongly biased equilibrium is the probable reason why no selective broadening was observed. This was further supported by the MM calculations, which predict an even less biased equilibrium for *2b* than for *1b*, and a barrier of 17.6 kJ mol^{-1}, although, as for *1b*, the barrier is probably somewhat underestimated.

The ^{1}H resonances of *1a* remain sharp down to −140 °C. This may be due either to a low barrier or to a strong preponderance of one conformation or both. The MM calculations predict the *syn* form of *1a* (Fig. 3) to be essentially the same as for *1b*, only 0.4 kJ mol^{-1} higher in energy than the global *anti* minimum. The *anti* form has two minima, a local one similar to that in *1b* ($\theta_1 = +163°$, $\theta_2 = +65°$) and a global one 1,5 kJ mol^{-1} lower ($\theta_1 = -126°$, $\theta_2 = +132°$). The two minima are separated by a barrier of 2.0 kJ mol^{-1}. The different geometries for the predicted global *anti* minimum of *1a* and the *anti* minimum of *1b* may explain why $\delta(H_\alpha)$ is lower in *1a* than in both the *syn* and *anti* forms of *1b* (Table 1). In the global *anti* minimum of *1a*, the angle between the N(1)-C(10)-H(17) plane and the indole plane is 50° which results in less deshielding of H_α, although the effect is partly reduced by the deshielding by the rotor phenyl ring. This, according to the calculations, is only 15° out of the plane spanned by H(17)-C(10)-C(11). The H-2 proton is deshielded both by the proximity of the rotor

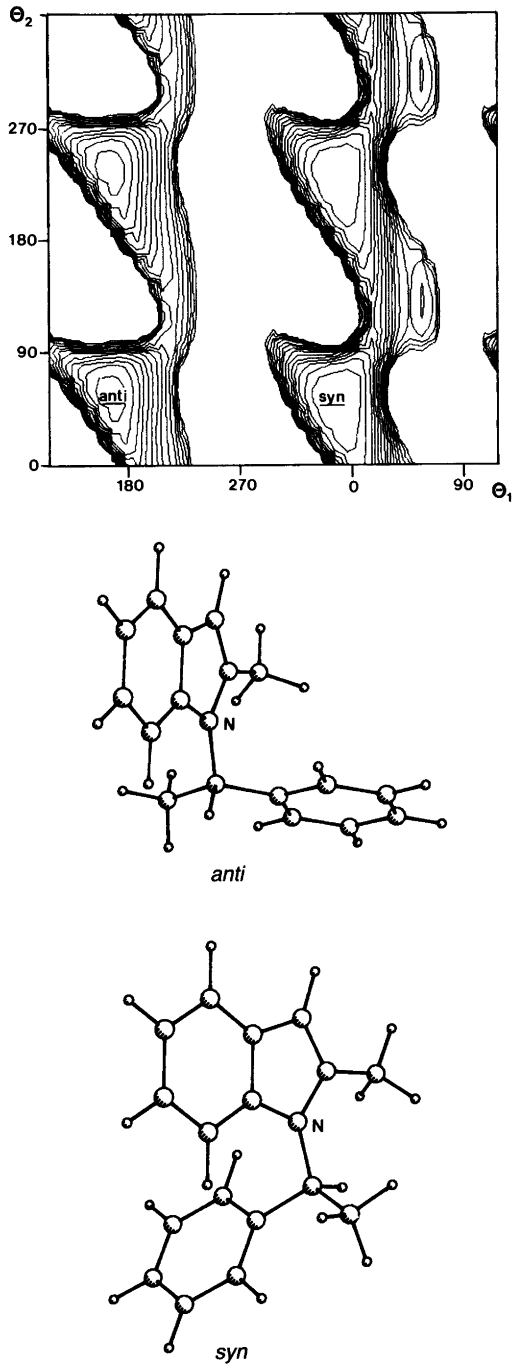

Fig. 2. Conformational energy map for *1b* and energy minimized structures. For definition θ_1 and θ_2, see text. Curves are omitted in high energy regions.

methyl group and by being almost in the plane of the rotor phenyl ring. Thus, the temperature dependence of δ(H-2) and lack of temperature dependence of $\delta(H_\alpha)$ are best interpreted in terms of a slightly biased *syn-anti* equilibrium, since an equilibrium between notable quantities of the two *anti* minima would probably lead to temperature dependence of $\delta(H_\alpha)$. Thus, based on the observed shifts and shift displacements and the close agreement between the calculated and experimental free energy difference for *1b*, we tentatively propose that there is an equilibrium with considerable amounts of both the *syn* and the *anti* rotamers with the latter as the major conformation. To estimate a barrier for *1a*, we can add the difference between the experimental and calculated barrier for *1b* (9.7 kJ mol^{-1}) to the calculated barrier for *1a* (15.2 kJ mol^{-1}). The resulting barrier, 24.9 kJ mol^{-1}, is, however, so high that a significant selective broadening of the H-2 resonance should be observed above −140°. However, with other chiral rotors, differences between 2-Me and 2-H compounds of 14–20 kJ mol^{-1} have been observed,[36] and it is possible that our estimated value for *1a* is too high.

The ^1H resonances of *2a* exhibit no selective broadening down to −140 °C, which was expected since the barrier ought to be lower than 20 kJ mol^{-1}. A *syn-anti* equilibrium similar to that anticipated for *1a* was assumed based on the following arguments: *i*) $\delta(H_\alpha)$ in *2a* appeared upfield of that in *2b*, i.e. the same relation is observed as between these resonances in *1a* and *1b*; *ii*) the H-2 proton resonance is shifted downfield with decreasing temperature; *iii*) the conformational map for *2a* is similar to that for *1a* with slight changes in the energy differences. The local *syn* ($\theta_1 = -11.3$, $\theta_2 = +60.1$) is 2.3 kJ mol^{-1} higher in energy than the global *anti* minimum ($\theta_1 = -125.6$, $\theta_2 = +126.5$). The local *anti* minimum ($\theta_1 = 166.6$, $\theta_2 = 69.8$) is 3.1 kJ mol^{-1} higher in energy than the global *anti* minimum and is separated from it by an almost negligible barrier. Actually, the local minimum was not seen, when constraining θ_1, distinct from that obtained for *1a* (Fig. 4), but only when the θ_1 restriction is removed the local minimum is obtained.

The absence of selective broadening in the ^1H NMR spectra of *1c* at low temperature is most likely due to a strongly biased equilibrium, since the barrier ought to be ca. 34 kJ mol^{-1}, estimated by subtracting the difference between the isopro-

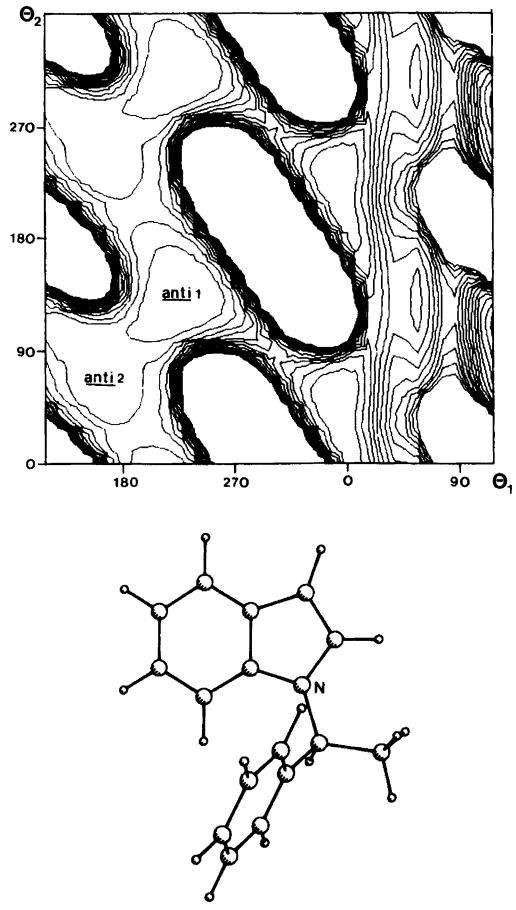

Fig. 3. Conformational energy map for *1a* and energy minimized structure.

pyl analogues from the barrier of *1b*. A notable downfield shift of the H_α resonance and a small upfield shift of the H-7 resonance with decreasing temperature can be explained by a conformational equilibrium involving the ester group. The near coplanarity of this with the indole ring is verified by the batochromic shifts of the UV transitions. The corresponding *N*-methylated 3-analogue *2c* exhibits neither exchange-broadened ^1H resonances, nor temperature-dependent shift displacements, which indicates a preponderant *syn* conformation. The situation is however complicated by the fact that the N-H precursor of *2c*,(*2c**), exhibits resonances of two forms in the ratio of 75:25 at −131 °C. The dynamic process was observed almost entirely on the H_α resonance, though some small changes in the aromatic region were also seen. The multitude and complexity of these signals prevented accurate analysis. The H_α resonance of the minor rotamer is upfield relative to that of the major rotamer, consistent with a *syn-anti* equilibrium with a dominant *syn* form. The alternative explanation for the splitting observed for *2c**, a slow rotation of the ester group, is less likely, since this group would be held preferentially in one position, nearly in the ring plane, by the NH...O = C hydrogen bond. A less mobile ester group also explains the rather high *syn-anti* barrier, and the similarity of the UV spectra of *2c* and *2c** can be ascribed to a cancellation of effects: the bathochromic effect of the *N*-methyl group[37] in *2c* balances the effect of increased coplanarity in *2c**.

No exchange broadening or notable temperature-dependent shift displacements of the ^1H resonances are observed for *1d*. This conforms with a strong prevalence of the *syn* structure (the *anti* must be very strained) and agrees with what was observed for the 1-isopropyl analogue. Further support for the assignment was obtained from the high $\delta(H_\alpha)$ value ascribed to the van der Waals effect in the encumbered environment of the bulky R^2 group. The small shift displacements may be due to an equilibrium between different conformations of the R^2 group, which, in turn, may result in slight differences in the conformation of the rotor in the *syn* form.

As for *1d*, no exchange effects are observed for the ^1H resonances of *2d*, and the temperature dependences of the shifts were similar, indicating a strong prevalence of the *syn* rotamer. However, the temperature dependence of the CD spectrum shows that *2d* is a more flexible molecule than inferred from the ^1H NMR data, and also more flexible than *1d*.

In the ^1H NMR spectra of *1e*, no indications of slow rotation are observed, whereas *2e* shows resonances of two forms in the ratio of 56:44 at −143 °C, separated by a barrier of 33.3 kJ mol^{-1}. In contrast to what was found for *1b*, $\delta(H_\alpha)$ has the same value for the two rotamers, whereas all indole resonances except for that of the *N*-methyl group are doubled, as is the rotor methyl resonance, although with small splittings. The MM calculations for *2e* predict the lowest *syn* form to be 0.65 to 3.0 kJ mol^{-1} lower in energy than the lowest *anti* form with a barrier of 15.5–21.8 kJ

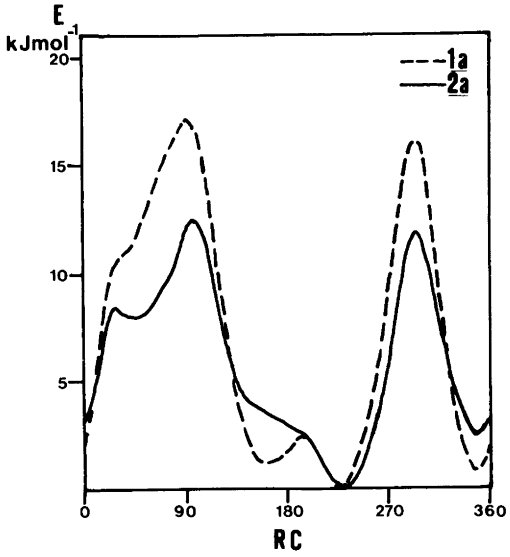

Fig. 4. Potential energy curve for the rotation of the 1-phenylethyl group (θ_1) for *1a* and *2a*.

mol^{-1} (Table 4), when the V_2 term in the torsional parameters for C(2)-C(18) bond is varied between 7.5 and 13 kJ mol^{-1}. (A small free energy difference corresponds to a small activation energy.) There are several local minima in the *anti* conformation, 2.8 to 4.6 kJ mol^{-1} higher in energy than the lowest *anti* minimum. For *1e,* the lowest *syn* minimum is calculated as 2.6 to 6.4 kJ mol^{-1} lower than the lowest *anti* minimum, depending on the magnitude of V_2. The other minima in the *anti* form are between 2.7 and 4.6 kJ mol^{-1} higher in energy than the lowest *anti* minimum. The reaction coordinate for the rotation of the isopropenyl group around the C(2)-C(18) bond, with the chiral rotor in the *syn* region, but free to relax, reveals two minima for *2e* of almost equal energy ($\theta_3 = -50$, $+130°$) (Table 5) with a barrier for interconversion ($\theta_3 = 180°$) of 35.6 kJ mol^{-1} if $V_2 = 9.2$ kJ mol^{-1} but lowered by approximately 10 kJ mol^{-1} if $V_2 = 13$ kJ mol^{-1}. The corresponding calculations for *1e* give a similar conformational map. When $V_2 = 9.2$ kJ mol^{-1}, the two lowest minima are essentially the same as for *2e,* with two additional minima ($\theta_3 = -140$, $+46°$) only 2.7 and 3.6 kJ mol^{-1} higher in energy respectively, and a barrier ($\theta_3 = 180°$) of 12.8 kJ mol^{-1}. If $V_2 = 13$ kJ mol^{-1}, the relative energies of the minima are approximately maintained, though they are slightly shifted towards coplanarity. The lowest barrier (14.8 kJ mol^{-1}) is obtained when $\theta_3 = 10°$. The accuracy of the barrier for the rotation of the isopropenyl group is hard to estimate; the π-electron calculations are excluded and the variations in the bond order are therefore not properly represented. The choice of the V_2 term is important also for the energy difference in the *syn-anti* equilibrium. Despite this and other deficiencies in the force field, it is unlikely that the barrier for the isopropenyl rotation is lower than the lowest calculated. Thus, we conclude that there are two plausible explanations for the equilibrium observed by ^1H NMR for *2e* and not observed for *1e.* The more likely is a conformational equilibrium of the isopropenyl group where either the methyl or the ethenyl part are on the same side of the indole plane as the phenyl ring with the chiral rotor in the *syn* region. The non-splitting of the H_α resonance of *2e* is perhaps most readily explained by this. The splitting of the resonances of the aromatic protons in the two rotamers may be due to slightly different conformations within the *syn* form, though not revealed by the calculations. Furthermore, the calculated energy difference and barrier are close to the experimental values. The reason for not observing such an equilibrium for *1e* is obvious – the barrier is too low. The other explanation, a *syn-anti* equilibrium of *2e,* cannot be excluded although the calculated barrier is 11.7 to 15.8 kJ mol^{-1} lower than that experimentally observed, where the largest difference of the barriers corresponds to the smallest free energy difference between the *syn* and *anti* forms. The small shift differences between all signals of the rotamers are also arguments against a *syn-anti* equilibrium. If, however, the observed equilibrium actually were a *syn-anti* equilibrium, the absence of exchange-broadening of the resonances of *1e* is most likely due to a strongly biased equilibrium since, according to the MM calculations, the barrier to *syn-anti* interconversion should be higher for *1e* than for *2e.* Finally, we must emphasize that the assignments of the observated equilibrium to one or to one other proposed equilibrium does not rule out the possibility that the rejected process exists, but that the barrier is too low to allow detection.

Ultraviolet spectra. The electronic transitions in the indole chromophore have been intensely studied in view of their importance for investi-

gations of the occurrence and behaviour of tryptophan residues in proteins. Four transitions have been observed between 190 and 300 nm in indole and its alkyl derivatives. They are in the notation of Platt[38] transitions to the ^1L_b, ^1L_a, ^1B_b and ^1B_a states, and they display different fine structure and sensitivity to substituents and solvent polarity. The ^1L_b and ^1L_a bands fall in the region 240–300 nm and overlap partly. Mainly due to the work of Strickland *et al.*,[28,39–41] the properties of these transitions are now fairly well known. In unsubstituted indole, the ^1L_b transition gives rise to a succession of weak but distinct vibrational bands, starting with the strongest at 287 nm (hydrocarbon solvent) and falling off towards shorter wavelengths. These bands undergo red shift on alkyl substitution, most notably in position 5, and they are only slightly sensitive to solvent polarity. The ^1L_a band is stronger and broader, with less discernable fine structure, with a maximum at 266.5 nm. It is also shifted to the red by alkyl substitution, although it is only slightly sensitive to substituents in position 5. It undergoes notable red shifts with increasing solvent polarity.

The transitions to the ^1B_b and ^1B_a states have been assigned by Auer[42] to strong bands at *ca.* 220 and 195 nm in tryptophan derivatives. The former may show some fine structure, and both undergo red shifts with increasing solvent polarity. Their substituent sensitivity is less well known than for the ^1L_b and ^1L_a transitions. These four bands should be observed in the UV spectra of the 1- and 3-(1-phenylethyl)indoles *1* and *2*, together with bands of the transitions to the ^1L_b and ^1L_a states of the benzene chromophore, while the transition to the ^1B_b and ^1B_a states of the benzene chromophore are below the observed wavelength region. The benzene ^1L_b transition is observed as a weak band with vibrational fine structure in the region 260–270 nm; the ^1L_a band is centered around 210 nm. Wavelengths and ε values for extremes are given in Table 9.

CD spectra. The absolute configuration for the compounds included in this study is not known *a priori*, except for *1f* and *1g*, which have the (*S*) configuration. For the compounds with unknown configuration, the enantiomer first eluted in the chromatographic separation[5] (E_1) was used in the CD measurements. Wavelengths and Δε values for extreme points are given in Table 10.

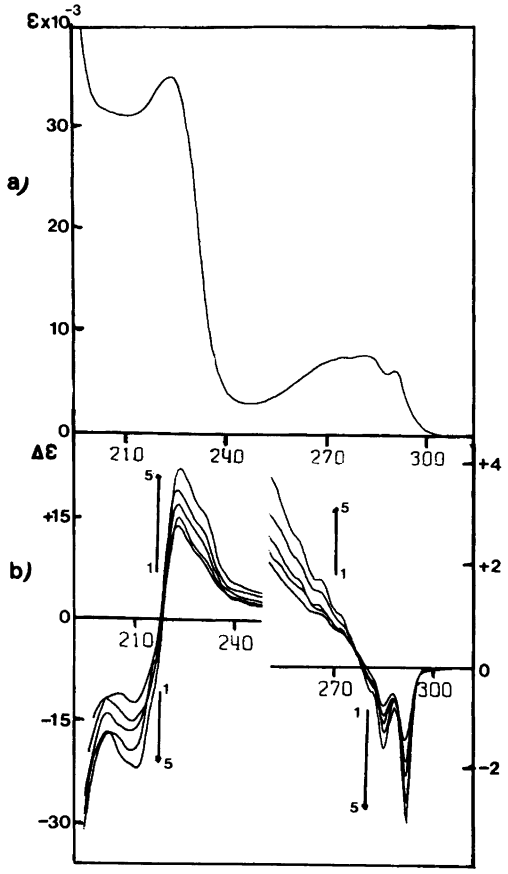

Fig. 5. a) Ultraviolet spectrum of *1b* in methanol. b) CD spectra of *1b* in methanol at 1) +22, 2) −12, 3) −36, 4) −67 and 5) −96 °C.

Based on the similarity of the CD spectra of *1b* (Fig. 5) and *1d* (Fig. 7) to that of *1g* (Fig. 6) we can safely conclude that the E_1 enantiomers of *1b* and *1d* also have the *S* conformation, and since E_1 of *1d* is transformed into *1e* without affecting the chiral center, we can conclude that the depicted CD spectra of *1e* (Fig. 8) are of the *S* configuration. For the other compounds no safe experimental assignment of absolute configuration can be made. Albeit chromatographic elution orders have been used to predict absolute configuration, the chiral recognition mechanism of microcrystalline tricetylcellulose is still insufficiently known to allow this in our case. As mentioned by other workers[43,44] the elution order with respect to configuration may be reversed by a conformational change. For the same reasons as for *1d* and *1e*, the E_1 enantiomers of *2d* and *2e* can be as-

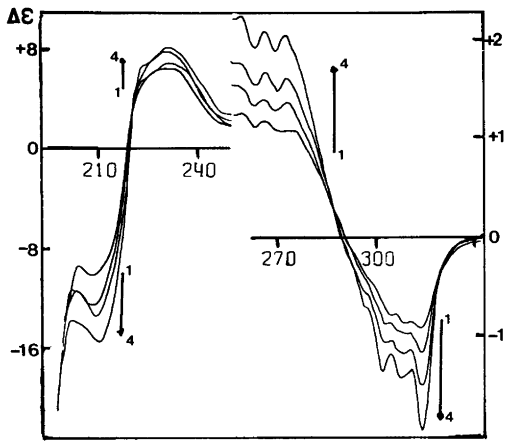

Fig. 6. CD spectra of *1g* in methanol at 1) +23, 2) −19, 3) −57 and 4) −95 °C.

signed to the same configuration. Since the NMR data for *1b* and *1g* gave unambiguous conformational results and their absolute configurations are known, it is appropriate to begin the discussion and interpretation of the CD spectra with these two compounds.

The CD spectrum of (*S*)-*1b* (Fig. 5, Table 10) at ambient temperature exhibits two weak but distinct negative bands at 286 and 292 nm in relative intensity typical for the indole ^1L_b transition, while for *1g* the corresponding band centered around 310 nm is broader and has less fine structure. The strong batochromic effect of the 5-methoxy substituent on this band has previously been observed by Strickland and Billups.[28] The weak positive band centered around 265 nm for both *1b* and *1g* was assigned to the indole ^1L_a transition. The benzene ^1L_b band is seen as vibrational fine structure around 260 nm, superimposed on the indole ^1L_a band, so weak that nothing can be said about its actual sign. The bisignate CD curve of *1b* between 200 and 230 nm is composed of a strong positive indole ^1B_b band at 222 nm and a negative benzene ^1L_a band at 209 nm. At shorter wavelength, there is a negative minimum around 200 nm which may indicate that the indole ^1B_a band is positive, since no corresponding minimum is seen in the UV curve (Fig. 5, Table 9). The spectrum of *1g* looks very similar in this region with a positive indole ^1B_b band at 231 nm and a negative benzene ^1L_a band at 208 nm.

According to the NMR study, the conformational equilibria of *1b* and *1g* are very similar, *ca.* 70:30 in favour of the *syn* form at ambient temperature, assuming negligible entropy difference between the *syn* and *anti* rotamer. The temperature dependence of the CD spectrum of *1b*, going from ambient temperature to −96 °C, also reveals the existence of a conformational equilibrium (Fig. 5). The negative maxima of the indole ^1L_b band become further negative by a factor of 2 and Δε of the positive ^1B_b band increases from 14 to 22. The indole ^1L_a band is partly obscured by overlap with the ^1B_b band, and its temperature dependence is difficult to evaluate, but an increase in the positive Δε in this region is observed. The benzene ^1L_a transition exhibits temperature dependence similar to the indole ^1B_b band but of opposite sign (Δε −12.4 at 22 °C, −22.1 at −96 °C), which corroborates the impression that the couplet character of the indole ^1B_b and benzene ^1L_a bands mainly originates from the coupling between these two transitions, at least in the major conformation. The spectra exhibit isosbestic points at 277 and 217 nm, which indicates that the observed equilibrium is between two forms only: a *syn* and an *anti* rotamer, in agreement with the MM calculations. From the observed temperature dependence, we can consequently conclude that the rotational strengths of the indole ^1L_b, ^1L_a, ^1B_b and benzene

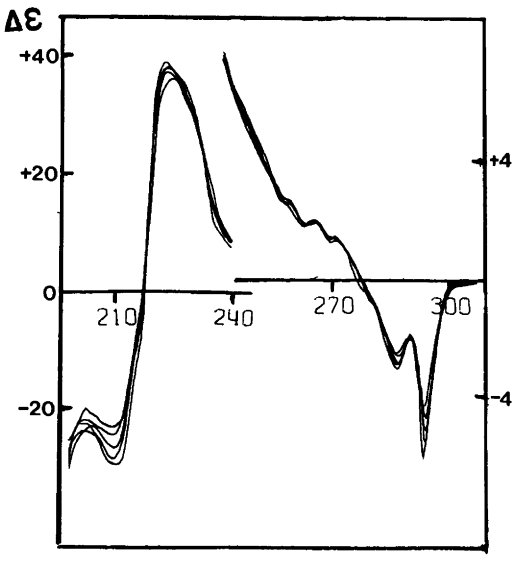

Fig. 7. CD spectra of *1d* in methanol at 1) +21, 2) −3, 3) −30, 4) −56 and 5) −89 °C.

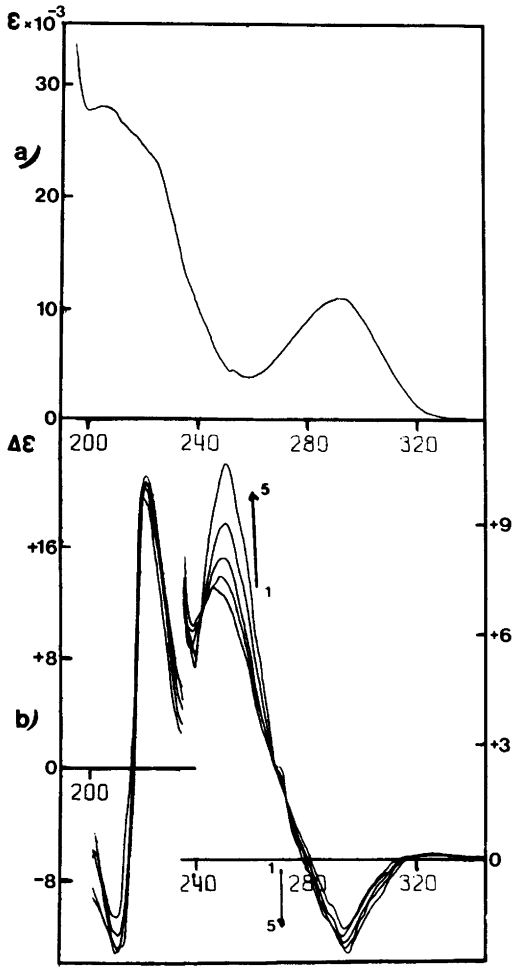

Fig. 8. a) Ultraviolet spectrum of *1e* in methanol. b) CD spectra of *1e* in methanol at 1) +21, 2) −3, 3) −26, 4) −55 and 5) −92 °C.

^1L_a transitions are negative, positive, positive and negative, respectively in the *syn* form. By use of eqn. (3),[45] and $\Delta G°_{syn\text{-}anti} = 2.0$ kJ mol^{-1} obtained from the NMR studies and measuring $\Delta\varepsilon_{obs}$ for each transition at two different temperatures we come to the conclusion that the signs of the rotational strengths of the indole ^1L_b and ^1B_b and the benzene ^1L_a transitions are opposite in the *syn* and *anti* rotamers.

$$\Delta\varepsilon_{obs} = (\Delta\varepsilon_{syn} - \Delta\varepsilon_{anti})(1 + e^{-\Delta G°/RT})^{-1} + \Delta\varepsilon_{anti} \quad (3)$$

The sign of the indole ^1L_a band in the *anti* form was not evaluated due to the overlap mentioned above. However, the development of the curve in the region 265–275 nm is not contradictory to a negative ^1L_a transition in the *anti* form. The temperature dependence of the spectrum of *1g* (Fig. 6) deviates slightly from that of *1b*. At −95 °C, the negative indole ^1L_b band increases by the same magnitude as for *1b* with raised vibrational fine structure. The indole ^1L_a band increases considerably more in *1g* than in *1b*, almost by a factor of 2, while the indole ^1B_b increases by only approximately 25 % and the benzene ^1L_a band by 50 %. The temperature dependence reveals that the signs of the transitions in the *syn* form are the same as for the transitions in the spectra at ambient temperature. Since $\Delta G°$ for the *syn-anti* equilibrium is the same as for *1b*, the signs of the transitions in the *anti* form are opposite to those in the *syn* form. However, the rotational strength of the indole ^1B_b transition in the *anti* form is rather small.

Concerning the theoretical calculations for *1b* there is a fairly good agreement for the indole ^1L_b and ^1L_a transitions. In the *syn* rotamer of the *S* form, the rotational strength of the indole ^1L_b transition, $\boldsymbol{R}(^1L_b)$, is predicted to be negative and $\boldsymbol{R}(^1L_a)$ to be positive, while the opposite signs were predicted for the *anti* form (Table 8) in accord with the experimental observations. Besides, the calculations reproduce the larger experimental dissymmetry factor[46] $\Delta\varepsilon/\varepsilon$ for the indole ^1L_b than for the ^1L_a transition. The results for the other transitions are less satisfactory. Although indole $\boldsymbol{R}(^1B_b)$ is calculated to be positive ($\boldsymbol{R}$ +0.3) in the *syn* form, in agreement with experiment, the value for the *anti* form is calculated to be strongly negative ($\boldsymbol{R}$ −3.2). This, in combination with $\Delta G°_{syn\text{-}anti} = 2.0$ kJ mol^{-1}, should give a negative ^1B_b band at room temperature, whereas it was found to be positive. Variation of the polarization of the ^1B_b transition from +55 to −15° (CNDO/S +5.8°) did not give rotational strengths, which reproduced the observed $\boldsymbol{R}(^1B_b)$ value. The calculated benzene $\boldsymbol{R}(^1L_a)$ values ($\boldsymbol{R}_{syn}$ −0.7, $\boldsymbol{R}_{anti}$ +0.57) do at least qualitatively reproduce the observed Cotton effect of this transition, but this is probably merely a coincidence, since the coupling between the indole ^1B_b and benzene ^1L_a transitions seems to be the most important contribution to the rotational strengths of these transitions.

The CD spectrum of *1d* (Fig. 7) does not exhi-

bit any significant temperature dependence, except for the sharpening of the indole ^1L_b bands, and the spectrum strongly resembles that of *1b*, but with increased positive and negative maxima for all transitions. This is in agreement with a strongly dominant *syn* form of *1d*, as indicated by the NMR studies. A change in population of vibrational levels in the ground state at low temperature is probably responsible for the sharpening of these bands; the area under the bands is essentially unchanged.

With the exception of a negative band at 294 nm and a weak positive band at 247 nm, the spectrum of *1e* (Fig. 8) is also quite insensitive to temperature changes. Furthermore the spectrum is, except for the band at 247 nm, similar to that of *1d*, although the intensities are lower. The UV spectrum of *1e* (Fig. 8, Table 9) shows some influence from conjugation. The most prominent deviation from the spectra of *1a*, *1b* (Fig. 5) and *1d* is the decrease of the indole ^1B_b band, but an increase in the sum of the oscillator strengths of the indole ^1L_b and ^1L_a transitions is also observed (Table 9). The decrease in oscillator strength of the ^1B_b transition may explain at least part of the decrease in the indole $\boldsymbol{R}(^1B_b)$ and benzene $\boldsymbol{R}(^1L_a)$ values of *1e* compared to those of *1d*. The temperature dependence in the 240–320 nm region, with two distinct isosbestic points at 242 and 270 nm in the CD spectrum clearly reveals a conformational process in *1e*. A plausible explanation, supported by the MM calculations, is a rotation of the 2-isopropenyl group with the chiral rotor in the *syn* region.

The relatively strong negative band at 300 nm, which increases with decreasing temperature, is assigned to the indole ^1L_b and the very weak positive one at 322 nm to the ^1L_a transition. A possible rationalization is that a positive ^1L_a band, shifted batochromically by the 2-substituent,[41] is cancelled by a stronger negative ^1L_b band, leaving the weak band at 322 nm as the only observable residue. In this way, the relation between the signs of these transitions is the same as in *1b* and *1d*.

The most striking feature in the spectrum is the temperature-dependent band at 247 nm. Its origin is not obvious. The bands due to the normal transitions are found in the usual wavelength regions. A possibility, which has been suggested for other indoles,[27,42] is the ^1C transition proposed by Platt[38] for naphthalene and polyacenes. It is symmetry-forbidden in these compounds, but it may be allowed in indole, although it is not strong enough to be observed in the UV spectrum. There are indications of a shoulder in the region 225–240 nm in the CD spectra of several of our compounds, and we tentatively propose that these have the same origin as the prominent 247 nm band of *1e*. The strong temperature dependence shows that the $\boldsymbol{R}$ value of this transition is more sensitive to the orientation of the 2-isopropenyl group than the others.

The CD spectrum of the E_1 enantiomer of *1a* (Fig. 9) shows a shape somewhat similar to that of *1b*, with a negative indole ^1L_b transition seen as distinct peaks at 286 and 293 nm, a positive indole ^1B_b band at 224 nm and a negative benzene ^1L_a band at 206 nm. The only exception is the indole ^1L_a transition, seen as a rather weak negative band around 280 nm partly overlapping the ^1L_b band. The temperature dependence reveals the existence of a conformational process; in all cases, the intensity of the bands increases with decreasing temperature. This implies that the signs of the indole ^1L_b, ^1L_a, ^1B_b and benzene ^1L_a transitions are negative, negative, positive and negative, respectively in the major form.

The rotational strength calculations for the *S* configuration of *1a* predict positive indole $\boldsymbol{R}(^1L_b)$ in the *anti* forms and negative in the *syn* form, while the reverse holds for the ^1L_a transition. This is in conflict with the experimental observations, where the ^1L_b and ^1L_a transitions have the same sign in the major form. However, as for *1b*, *1d* and *1e*, the dissymmetry factor of the ^1L_a transition is small compared to that of ^1L_b. This is reproduced by the calculations. Furthermore, there are nodal lines not far from the *anti* minima in the $\boldsymbol{R}(^1L_a)$ map. Taking the uncertainties in the calculation of the rotational strengths into account, we can conclude that the $\boldsymbol{R}(^1L_a)$ values, in an area where the rotational strengths are small, are less reliable than the $\boldsymbol{R}(^1L_b)$ values, which in the whole *anti* region are calculated to be of the same sign and approximately the same magnitude. Based on this, and assuming that the global minimum is within the *anti* region, we tentatively propose that the E_1 enantiomer of *1a* has the *R* configuration, since the ^1L_b band is negative in the *anti* forms, opposite to the sign calculated for the *S* configuration. This is also the most straightforward way to explain the experimental observations. Neglecting the the-

oretical calculations, and assuming that the E_1 enantiomer has the *S* configuration and that the *syn-anti* equilibrium is as indicated by the NMR results and MM calculations, the rotational strength of the global *anti* form must have the same sign and probably larger magnitude than that of the *syn* form, for all transitions, except the indole ^1L_a – a coincidence which seems less probable, especially since the signs of most of the transitions in the *anti* form are opposite to those of the *syn* form for *1b*. The possibility that the E_1 enantiomer has the *S* configuration and that the *syn* form is the more stable, which could also explain the temperature dependence of the H-2 resonance in the ^{1}H NMR spectrum, is incompatible with the sign and temperature dependence of the indole ^1L_a band of *1a* compared to *1b*. Thus we conclude, based on both experimental results and theoretical calculations, that the E_1 enantiomer of *1a* has the *R* configuration.

The CD spectra of the E_1 enantiomers of *2a*, *2b* and *2d* (Figs. 10–12) closely resemble each other. In the spectrum of *2b* (Fig. 11) at ambient temperature, both the indole ^1L_b transition, seen as poorly resolved peaks at 293 and 300 nm, and the indole ^1L_a transition centered around 276 nm exhibit negative Cotton effects, while the indole ^1B_b and ^1B_a bands at 224 and approximately 200 nm, respectively, are positive. The absolute magnitudes of these bands increase considerably with decreasing temperature. The benzene ^1L_a transition is a weak negative band at 207 nm but becomes a positive minimum at lower temperature due to overlap by the strong indole ^1B_b and ^1B_a transitions on both sides of it. Similarly, the negative indole ^1L_b and ^1L_a transitions and the positive indole ^1B_b transition of *2a* and *2d* increase in rotational strength with decreasing temperature, although the temperature dependence of the ^1B_b transition is not as strong as for *2b*. At shorter wavelength, the similarities are less pronounced. In *2a*, the indole ^1B_a transition at 199 nm is positive and increases slightly at lower temperature, while the positive band at 201 nm becomes a negative minimum for *2d* at lower temperature. The assumed benzene ^1L_a band at 208 nm is a positive minimum for *2a* at ambient temperature but becomes a negative maximum at lower temperature. This for *2d* already occurs at room temperature with increasing negative rotational strength at low temperature. The CD spectrum of *2e* (Fig. 13) is similar to those of *2a*, *2b* and *2d* and exhibits a pronounced temperature dependence. The negative indole ^1L_b and ^1L_a transitions give rise to only one band with the maximum at 299 nm, and the only vibrational fine structure, at 266 and 271 nm, is due to the benzene ^1L_b transition. The positive band with the maximum at 223 nm, at ambient temperature, which increases with decreasing temperature, is probably due to the indole ^1B_b transition. There is also a shoulder at 226 nm which in-

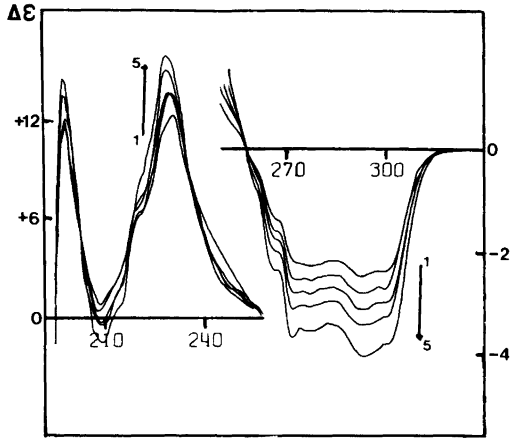

Fig. 10. CD spectra of *2a* in methanol at 1) +23, 2) −11, 3) −30, 4) −53 and 5) −88 °C.

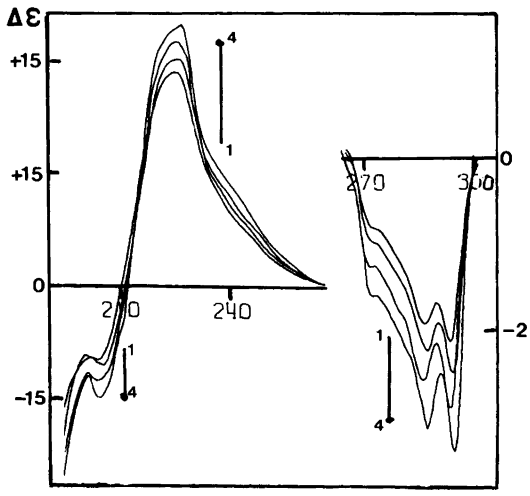

Fig. 9. CD spectra of *1a* in methanol at 1) +22, 2) −19, 3) −54 and 4) −96 °C.

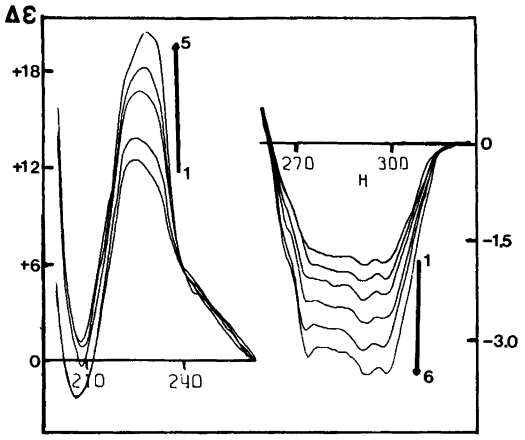

Fig. 11. CD spectra of *2b* in methanol at 1) +23, 2) −2, 3) −26, 4) −51, 5) −75 and 6) −97 °C.

creases considerably and becomes a separate band at 230 nm at lower temperature. The benzene ^1L_a transition gives a weak negative band with very minor temperature dependence, while the positive indole ^1B_a band at 200 nm decreases at lower temperature.

Thus, we can conclude that the temperature dependences of *2a, 2b, 2d* and *2e,* which are similar down to 215 nm, reveal conformational processes. The most striking observation is the pronounced temperature dependence of the spectrum of *2d,* which is in sharp contrast to that of *1d,* and also contrary to our earlier assumption based on NMR data that *2d* is a rather rigid molecule. The isosbestic points in the spectra of all four compounds in the long wavelength region indicate that the conformational equilibria are essentially between two forms. An analysis of the $\Delta\varepsilon_{obs}$ of the indole ^1L_a and ^1L_b bands at a specific wavelength according to Wood *et al.*[45] was therefore regarded as feasible. In addition, the same analysis was also applied to the CD spectra of *1b, 1f* and *1g.* The results from the calculations are shown in Table 11. Despite the fact that the values for $\Delta G°$ are not considered to be precise to more than ±1 kJ mol^{-1}, the trend in the absolute $\Delta G°$ values is compatible with the MM calculations and the NMR results.

The $\Delta G°_{syn\text{-}anti}$ value for *2b,* +2.1 kJ mol^{-1}, agrees well with the interpretation of the NMR data. If $\Delta G°$ were as low as 0.6 kJ mol^{-1}, as found by the MM calculations, p_{syn} would increase only

Table 11. Free energy difference ($\Delta G°$) for compounds *1b, 1f, 1g, 2a, 2b, 2d* and *2e* determined from the temperature dependence of the CD spectrum.

Compounds	$\Delta G°_{(maj.\rightarrow min.)}$/kJ mol^{-1}
1b	2.4±1.0 (1.97)[a]
1f	3.1±1.0 (3.73)
1g	1.7±1.0 (1.90)
2a	3.7±1.0
2b	2.1±1.0
2d	3.6±1.0
2e	2.7±1.0 (0.25)

[a]The values in parentheses are those obtained by the D NMR technique.

by a factor of 1.06 from +20 to −85 °C, which could not give rise to the observed temperature effects on the CD spectrum without assuming unreasonably high $R(^1L_a)$ values for both the *syn* and the *anti* forms of *2b* compared to those of *2a* and *2d.* The possibility of a preponderant *anti* form of *2b,* based on the $\Delta G°$ value from the CD analysis cannot be entirely dismissed. However, considering the NMR data and the MM calculations, this interpretation is regarded as less probable.

A dominating *syn* form of *2b* implies that the

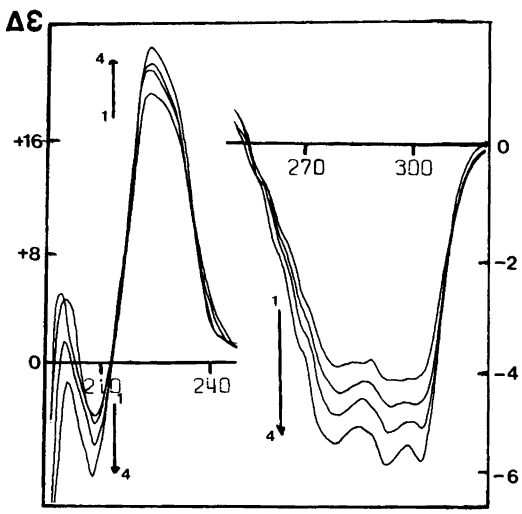

Fig. 12. CD spectra of *2d* in methanol at 1) +22, 2) −18, 3) −53 and 4) −92 °C.

sign of $\Delta G^{\circ}_{syn \rightarrow anti}$ of *2a* is negative, i.e. the *anti* rotamer is the major one, since the absolute ΔG° value for *2a* is larger than that for *2b* (Table 11). As earlier suggested, the distinct isosbestic point at 258 nm in this CD spectrum indicates that *2a* contains mainly two conformers. This corroborates the MM calculations that the barrier between the two *anti* minima is negligible and the whole *anti* region for *2a* can be treated as one minimum.

Which conformational process is then responsible for the observed temperature dependence of the CD spectrum of *2d*? The close resemblance, at least down to 215 nm, to the spectra of *2b* and the $\Delta G^{\circ}_{syn \rightarrow anti}$ = +3.6 kJ mol^{-1} obtained from the temperature dependence indicate a similar *syn-anti* equilibrium for *2d* as suggested for *2b*, though more biased in favour of the *syn* rotamer. This is contrary to the NMR results, since one would expect a temperature-dependent shift of the H_{α} resonance. Furthermore, the evident differences between the CD spectra of *2b* and *2d* from 215 to 200 nm are hard to explain. assuming that the rotational strengths of the benzene ^1L_a and indole ^1B_a transitions in the dominating *syn* form are essentially the same for the two compounds, which seems reasonable. An explanation which possibly may account for the temperature dependence is an equilibrium between two rotamers with different orientations of the 2-(1-methyl-1-hydroxyethyl) group and therefore different conformations of the chiral rotor within the *syn* region. However, this seems less probable, since a similar equilibrium should hold for *1d*, for which no temperature dependence of the CD spectrum is observed. Thus, despite the evident discrepancies in the present model, the most viable explanation for the temperature dependence of the CD spectrum of *2d* is a *syn-anti* equilibrium with a preponderant *syn* form.

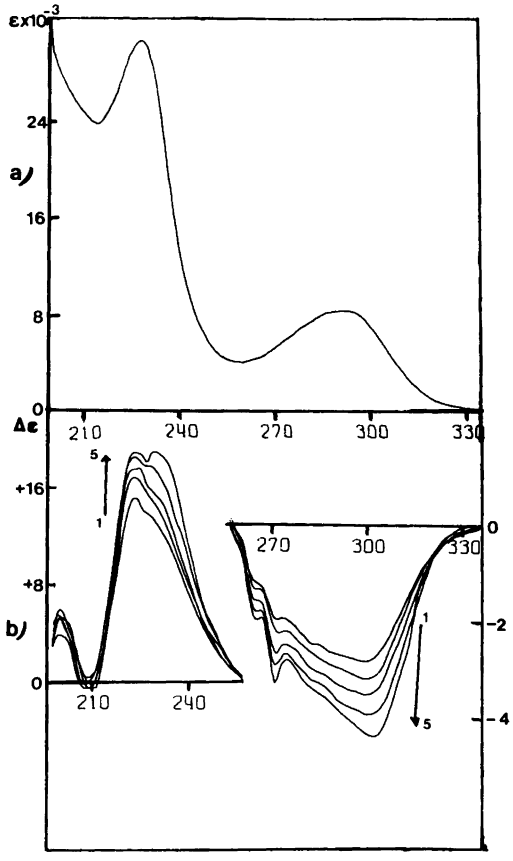

Fig. 13. a) Ultraviolet spectrum of *2e* in methanol. b) CD spectra of *2e* in methanol at 1) +23, 2) −6, 3) −31, 4) −60 and 5) −92 °C.

According to the MM calculations, there are two plausible conformational processes for *2e*, the *syn-anti* exchange and a rotation of the 2-isopropenyl group with the chiral rotor in the *syn* region. The small ΔG° value (0.25 kJ mol^{-1}) for the equilibrium observed with the D NMR technique, which is close to the ΔE° value calculated by MM for the equilibrium of the isopropenyl group, corresponds only to a change of p_{major} by a factor of 1.03 in the observed temperature interval, assuming negligible entropy difference between the rotamers. From this, we can conclude that the observed temperature dependence can hardly be explained by this process, no matter whether it is a *syn-anti* equilibrium or an equilibrium of the isopropenyl group, particularly not the latter, since the conformations of the chiral rotor are calculated to be almost the same for the two forms of the isopropenyl group. Instead, a more biased *syn-anti* equilibrium as proposed for *2b*, with the *syn* rotamer as the more stable conformation, is the most likely explanation to the observed temperature dependence. This is supported by the ΔG° value (+2.7 kJ mol^{-1}) from the CD analysis, which is close to the higher limit of the energy difference for the *syn* and *anti* rotamers as predicted by the force-field calculations. Thus, we propose that the equilibrium observed by the DNMR technique for *2e* is not the

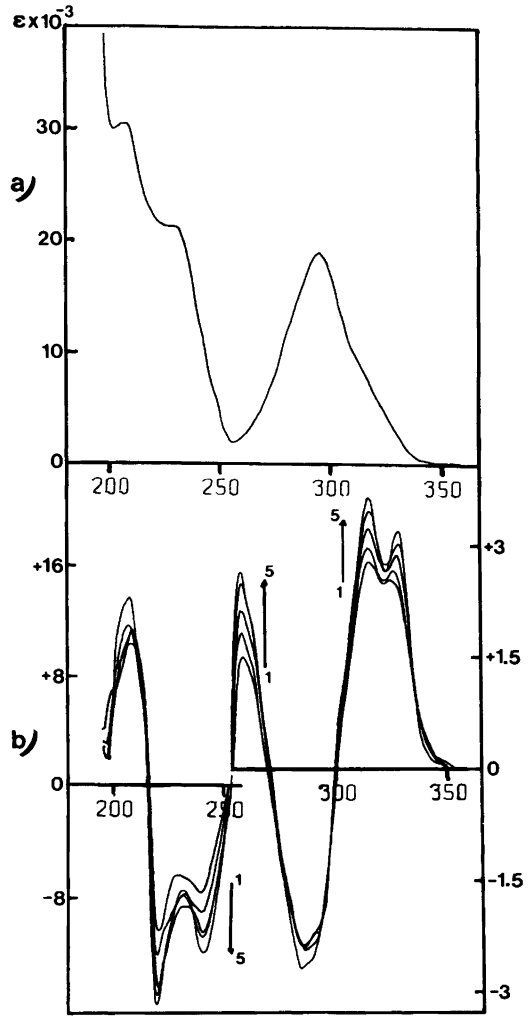

Fig. 14. a) Ultraviolet spectrum of *1c* in methanol. b) CD spectra of *1c* in methanol at 1) +22, 2) −3, 3) −27, 4) −49 and 5) −81 °C.

same equilibrium which is responsible for the major part of the temperature dependence in the CD spectrum; instead, this is due to a *syn-anti* equilibrium.

The extra band around 250 nm for *1e* has a counterpart in the CD spectrum of *2e*. An inflection point at 226 nm at room temperature develops into a distinct positive peak at 230 nm at lower temperature. We propose that the appearance of two bands at 223 and 230 nm is due to two transitions in the indole chromophore, the ^1B_b transition overlapped by a ^1C transition. The blue shift and smaller rotational strength of the proposed ^1C transition of *2e* compared to that of *1e* is probably due to decreased influence of the 2-isopropenyl group on the electronic transition in the indole chromophore of *2e*, which in turn is caused by decreased conjugation in *2e* compared to *1e* as predicted by the MM calculations. The decreased conjugation of the isopropenyl group is also seen in the UV spectrum of *2e* (Fig. 13), which shows only minor deviation from those of *2a*, *2b* and *2d*. The increased intensity of the ^1B_b band compared to that of *1e* is particularly worth mentioning.

Assuming that the proposed *syn-anti* equilibrium of *2b* is correct, i.e. that the *syn* form dominates, the temperature dependence of the CD spectrum implies that the indole $\boldsymbol{R}(^1L_b)$ and $\boldsymbol{R}(^1L_a)$ are negative and the indole $\boldsymbol{R}(^1B_b)$ and $\boldsymbol{R}(^1B_a)$ are positive in the *syn* form, while the signs have to be the reversed for the indole ^1L_a and ^1B_b transitions in the *anti* form. Since no separation of ^1L_a and ^1L_b contributions is possible, nothing final can be said about the sign and magnitude of indole $\boldsymbol{R}(^1L_b)$ in the *anti* form. It may be negative and then of less magnitude than in the *syn* form, or it may be positive, in which case, nothing can be said about its magnitude. The same uncertainty holds for $\boldsymbol{R}(^1B_a)_{anti}$ due to overlap with neighbouring bands. The calculations predict negative $\boldsymbol{R}$ values for the four indole transitions in the *syn* form and positive $\boldsymbol{R}$ values except for the ^1L_b transition in the *anti* form, which is incompatible with the experimental observations. However, the input in the calculations of the indole $\boldsymbol{R}(^1B_b)$ and $\boldsymbol{R}(^1B_a)$ values has no experimental support and must be regarded as less reliable. Furthermore, the $\boldsymbol{R}(^1L_b)$ and $\boldsymbol{R}(^1L_a)$ values for *1b* are correctly reproduced with respect to sign and order of magnitude for the *syn* form and $\boldsymbol{R}(^1L_b)$ also for the *anti* form, whereas the experimental sign for $\boldsymbol{R}(^1L_a)$ in the *anti* form is uncertain. For *2b*, the calculated $\boldsymbol{R}(^1L_a)/\boldsymbol{R}(^1L_b)$ is approximately 60. The CD and UV curves in this region have similar shapes, indicating that $\boldsymbol{R}(^1L_a)/\boldsymbol{R}(^1L_b)$ is rather similar to the ratio of the oscillator strengths: *ca.* 10.[1] Thus, there is a reasonable correlation between the magnitudes of the calculated and experimental $\boldsymbol{R}$ values of the indole ^1L_b and ^1L_a transitions, which gives some confidence to the reliability of the former. Fortified by this, we propose that the E_I enantiomer

of *2b* has the *S* configuration. As a consequence of this discussion, it follows that E_1 of *2d* and naturally also *2e* most likely have the *S* configuration.

The calculated $\boldsymbol{R}(^1L_b)$ and $\boldsymbol{R}(^1L_a)$ for *2a* are both strongly positive in the global *anti* form while $\boldsymbol{R}(^1L_a)$ is slightly negative in the local *anti* minimum but close to a nodal line and negative in the *syn* form. As mentioned earlier, the isosbestic points indicated that we have only one *anti* minimum. However, one should emphasize that the $\boldsymbol{R}$ value for a broad flat minimum like the *anti* minimum is determined by the Boltzmann distribution over the accessible vibrational and, especially, the torsional states, which may show different $\boldsymbol{R}$ values, particularly if a nodal line should cross the low-energy region. The $\boldsymbol{R}(^1L_a)$ values in most parts around the global and local *anti* minima are positive, which means that $\boldsymbol{R}(^1L_a)$ in the *anti* minimum as a whole is predicted to be positive. Assuming, as for *2b*, that the sign of the calculated $\boldsymbol{R}(^1L_a)$ is correct in the *anti* form of *2a*, we tentatively propose that E_1 of *2a* has the *R* configuration. Further support for the assignment of E_1 of *1a* and *2a* to the *R* configuration and *2b* to the *S* configuration is obtained by comparison of the CD spectra of *1a*, *1b*, *2a* and *2b* with the corresponding 1- and 3-(1-*N*,*N*-dimethylcarbamoylethyl)indoles,[36] which all have known absolute configurations and exhibit similar *syn-anti* equilibria. Although the chromophores X in the chiral perturbers are very different, the similarities with respect to both sign and dissymmetry factor $\Delta\varepsilon/\varepsilon$ for the indole ^1L_b and ^1L_a bands are striking.

Attempts to obtain agreement between the theoretical and experimental $\boldsymbol{R}(^1B_b)$ values for *2b* were made by varying the polarization direction α for the indole ^1B_b transition. For α +35 to +55°, the sign was correctly reproduced, but with these α values, the sign for $\boldsymbol{R}(^1B_b)$ in the *syn* form of *1b* was opposite to the experimental value, *i.e.* there was no single α value and concomitant set of monopoles, obtained by the Lagrange multiplier technique, which gave satisfactory $\boldsymbol{R}(^1B_b)$ values for both *1b* and *2b*. An explanation, which may seem farfetched, is that the substituents on the indole ring have a strong influence on the polarization direction of the indole ^1B_b transition, although this is not shown by CNDO/S calculations.

The CD and UV spectra of the indole-2-carboxylates *1c*, *2c* and *2c** (Figs. 14–16), show strong influence of conjugation, consistent with near coplanarity of the ester group and the indole ring. Interestingly, there is a correlation in the region 270 to 330 nm between the CD spectra of *1b* and *1c* on the one hand and those of *2b* and *2c* and *2c** on the other. For *1c* (Fig. 14), the first strong band is positive with vibrational fine struc-

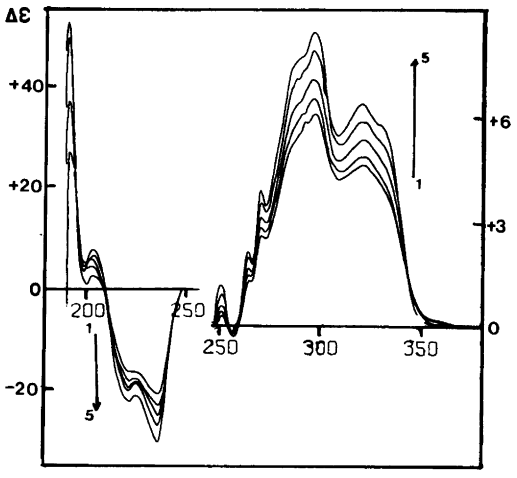

Fig. 15. CD spectra of *2c* in methanol at 1) +19, 2) −3, 3) −31, 4) −59 and 5) −92 °C.

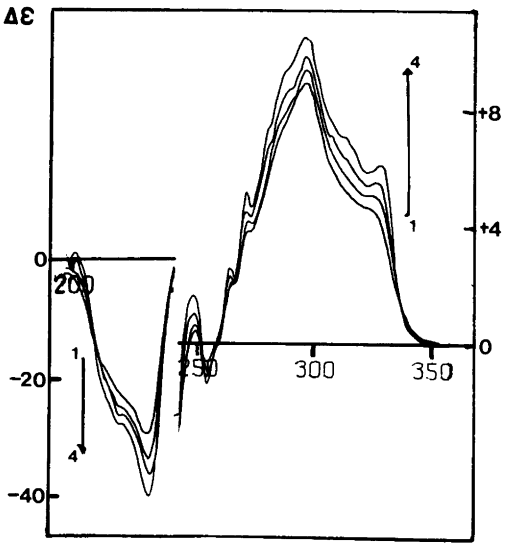

Fig. 16. CD spectra of *2c** in methanol at 1) +21, 2) −21, 3) −55 and 4) −95 °C.

ture at 314 and 325 nm, while the second weaker band at 285 nm has the reverse sign. Both bands increase slightly in intensity with decreasing temperature. Assuming that E_l of *1c* has the *R* configuration, this is in agreement with the signs of the indole $\boldsymbol{R}(^1L_b)$ and $\boldsymbol{R}(^1L_a)$ of *1b*. The two first bands of *2c* and *2c** (Figs. 15, 16) centered around 320 and 295 nm, respectively, are both positive, and the bands at 295 nm have the largest rotational strength. Assuming that E_l of *2c* and *2c** have the *R* configuration, this is in agreement with the signs and approximately also the magnitudes of the indole $\boldsymbol{R}(^1L_b)$ and $\boldsymbol{R}(^1L_a)$ values for *2b*. This may indicate that the polarizations of the indole ^1L_b and ^1L_a transitions of the indole-2-carboxylate derivatives are not very much influenced by the methoxycarbonyl group. The above discussion and tentative assignment of absolute configuration of *1c*, *2c* and *2c** holds, of course, only on condition that the *syn* rotamer is predominant in these compounds. The positive band at 258 nm in the CD spectrum of *1c*, which is close to a minimum in the corresponding UV spectrum, may arise from the earlier proposed ^1C transition. It can hardly be due to the benzene ^1L_b transition since it does not exhibit any fine structure.

All bands in the spectra of *2c* and *2c** show the same temperature dependence, which corroborates the earlier conclusion that *2c* has a similar *syn-anti* equilibrium as proposed for *2c** and that a low barrier and not a strongly biased equilibrium is responsible for the absence of selective exchange broadening of the ^{1}H NMR resonances of *2c*. The temperature dependence of most of the observed bands in the CD spectrum of *1c* may indicate a *syn-anti* equilibrium, which is less biased than inferred from the DNMR data, or it may be due to exchange of the ester group between two conformations. A safe conclusion is not possible at present.

The UV spectrum of *1f* (Fig. 17) exhibits some peculiar features. The indole ^1L_b band is blue-shifted compared to that of *1g*, while the indole ^1L_a transition is slightly red-shifted. Instead of an indole ^1B_b band in the region of 215–250 nm with a maximum around 225 nm, there are two bands in this region, a weaker with a maximum at 242.5 nm and a stronger with a maximum at 217 nm. The CD spectrum of *1f* (Fig. 17) shows strong resemblance to that of *1b* in the region of 200–240 nm, with a positive band at 222 nm and a negative benzene ^1L_a band at 209 nm, both increasing in rotational strength with decreasing temperature. In view of this, we tentatively assign the band at 217 nm in the UV spectrum to the indole ^1B_b transition, while the band at 242.5 nm, seen as a weak shoulder in the CD spectrum, is proposed for a ^1C transition modified by conjugation with the 3-methoxycarbonyl group. Thus, if the assignments are correct, the indole ^1B_b band of *1f* is also blue-shifted compared to that of *1g*. In the CD spectrum at longer wavelength, the benzene ^1L_b band is observed as a relatively strong nega-

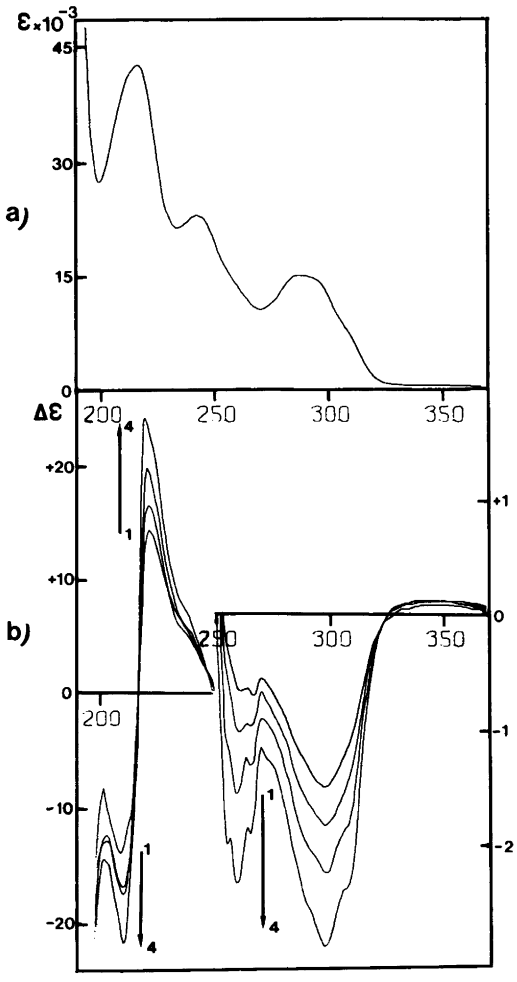

Fig. 17. a) Ultraviolet spectrum of *1f* in methanol. b) CD spectra of *1f* in methanol at 1) +22, 2) −18, 3) −53 and 4) −95 °C.

tive band with characteristic fine structure around 260 nm. The strong negative band with the maximum at 297 nm shows some fine structure with decreasing temperature, and can, in conformity with *1b*, probably be assigned to the indole ^1L_b band. The small positive band at 330 nm may be the rest of a weak positive ^1L_a band, which is cancelled by the benzene ^1L_b and indole ^1L_b bands at shorter wavelengths. The free energy difference of 3.1 kJ mol^{-1} for the *syn-anti* equilibrium obtained from the CD analysis is in fairly good agreement with the value obtained by the DNMR method (3.7 kJ mol^{-1}).

Conclusions

This study of 1- and 3-(1-phenylethyl)indoles shows the benefit of applying several methods to conformational analysis. Due to low barriers to the *syn-anti* interconversion, DNMR spectroscopy alone gives limited information, whereas the temperature dependence of the CD spectra for most of the compounds reveals dynamic equilibria. The existence of isosbestic points in many of the spectra indicates that only two forms are present, which presents the possibility for a determination of $\Delta G°$. For the 1-(1-phenylethyl)indoles with $R^2 = CH_3$, the $\Delta G°$ values from the CD analyses are in fairly good agreement with the values obtained by DNMR. For compound *2e*, an equilibrium between two almost equally populated sites ($\Delta G° = 0.25$ kJ mol^{-1}) is observed by DNMR, in agreement with the MM calculations identified as the rotation of the isopropenyl group, while the CD analysis probably reveals a more biased *syn-anti* equilibrium, also in agreement with the MM calculations.

The rotational strengths calculated for the indole ^1L_b and ^1L_a transitions for the minimum energy conformations predicted by the MM calculations for *1a, 1b, 2a* and *2b* are in fairly good agreement with respect to both the sign and dissymmetry factor and allow a tentative assignment of absolute configuration for most of the compounds in the series. These assignments are corroborated by comparison with other chiral indole derivatives with known absolute configuration.

The combined picture of the different methods indicates that the 1- and 3-(1-phenylethyl)indoles adopt similar *syn-anti* conformations as the corresponding isopropylindoles, and that the steric effect of the R^2 substituent appears in some cases to be smaller when the chiral rotor is in position 3 than when it is in position 1.

Acknowledgements. We thank Professor John Schellmann, University of Oregon at Eugene, for giving us access to his CD program and for much useful advice, Dr. Tommy Liljefors and Dr. Robert E. Carter for putting the facilities of the Computer Graphics Laboratory at our disposal, and T. Liljefors for advice with the MM calculations. We also thank Mr. Jan Glans for his excellent recording of numerous CD Spectra. Financial support from the Swedish Natural Science Research Council is gratefully acknowledged.

References

1. Yamamoto, Y. and Tanaka, J. *Bull. Chem. Soc. Jpn. 45* (1972) 1362.
2. Nilsson, I., Berg, U. and Sandström, J. *Acta Chem. Scand. B 38* (1984) 491.
3. Sundaralingam, M. *Biopolymers 7* (1969) 821.
4. Schellman, J. A. *Acc. Chem. Res. 1* (1968) 144.
5. Nilsson, I. and Isaksson, R. *Acta Chem. Scand. B 39* (1985) 531.
6. Fieser and Fieser. *Reagents for Organic Synthesis,* Wiley, New York 1967, p. 583.
7. Still, W. C., Kahn, M. and Mitra, A. *J. Org. Chem. 43* (1978) 2923.
8. Nystrom, R. F. and Berger, C. R. A. *J. Am. Chem. Soc. 80* (1958) 2896.
9. Sandström, J. *Dynamic NMR Spectroscopy,* Academic, London 1982, p. 68.
10. Lidén, A., Roussel, C., Liljefors, T., Chanon, M., Carter, R. E., Metzger, J. and Sandström, J. *J. Am. Chem. Soc. 98* (1976) 2853.
11. McConnell, H. M. *J. Chem. Phys. 28* (1958) 430.
12. Rogers, M. T. and Woodbrey, J. C. *J. Phys. Chem. 66* (1962) 540.
13. Lidén, A. and Sandström, J. *Tetrahedron 27* (1971) 2893.
14. Aue, W. P., Bartholdi, E. and Ernst, R. R. *J. Chem. Phys. 64* (1976) 2229.
15. Roschester, J., Berg, U., Pierrot, M. and Sandström, J. *J. Am. Chem. Soc. In press.*
16. Nordén, B. *Spectrochim. Acta 32A* (1976) 441.
17. Yergovich, T. W., Swift, G. W. and Kurata, F. *J. Chem. Eng. Data 16* (1971) 222.
18. Burkert, U. and Allinger, N. L. *Molecular Mechanics,* ACS Monograph 177, Washington, D.C. 1982.
19. Allinger, N. L. *J. Am. Chem. Soc. 99* (1977) 8127.
20. Allinger, N. L. and Yuh, Y. H. *Quantum Chemistry Program Exchange 11* (1980). Program No. 395.
21. Liljefors, T. *J. Mol. Graph. 1* (1983) 111.

22. Bayley, P. M., Nielsen, E. B. and Schellman, J. A. *J. Phys. Chem. 73* (1969) 228.
23. Kirkwood, J. G. *J. Chem. Phys. 5* (1937) 479.
24. Moffit, M. *J. Chem. Phys. 25* (1956) 467.
25. Guimon, C., Gonbeau, D. and Pfister-Guillouzo, G. *Tetrahedron 29* (1973) 3399.
26. Rizzo, V. and Schellman, J. A. *Biopolymers 23* (1984) 435.
27. Goux, W. J., Kadesch, T. R. and Hooker, Jr., T. M. *Biopolymers 15* (1976) 977.
28. Strickland, E. H. and Billups, C. *Biopolymers 12* (1973) 1989.
29. Shorygin, P. P., Petrukhov, V. A., Khomenko, A. Kh. and Chernyshev, E. A. *Russ. J. Phys. Chem. 42* (1968) 555.
30. Sklar, A. L. *Rev. Mod. Phys. 14* (1942) 232.
31. Platt, J. R. *J. Chem. Phys. 19* (1951) 263.
32. Mannschreck, A. and Ernst, L. *Chem. Ber. 104* (1971) 228.
33. Schaefer, T., Veregin, R. P., Laaitkainen, R., Sebastian, R., Marat, K. and Charlton, J. L. *Can. J. Chem. 60* (1982) 2611.
34. Roussel, C., Lidén, A., Chanon, M., Metzger, J. and Sandström, J. *J. Am. Chem. Soc. 98* (1976) 2847.
35. Pettersson, I. *Ph.D. Thesis,* University of Lund, 1984.
36. Nilsson, I., Berg, U., Liljefors, T. and Sandström, J. *To be published.*
37. Andrisan, V. and Vitali, T. *Gazz. Chim. Ital. 86* (1957) 949.
38. Platt, J. R. *J. Chem. Phys. 17* (1949) 484.
39. Strickland, E. H., Horwitz, J. and Billups, C. *Biochemistry 8* (1969) 3205.
40. Strickland, E. H., Horwitz, J. and Billups, C. *Biochemistry 9* (1970) 4914.
41. Strickland, E. H., Billups, C. and Kay, E. *Biochemistry 11* (1972) 3657.
42. Auer, H. E. *J. Am. Chem. Soc. 95* (1973) 3003.
43. Isaksson, R. and Roschester, J. *J. Org. Chem. 50* (1985) 2519.
44. Pirkle, W. H., Welch, C. J. and Mahler, G. S. J. *J. Org. Chem. 49* (1984) 2504.
45. Wood, W. W., Fickett, W. and Kirkwood, J. G. *J. Chem. Phys. 20* (1952) 561.
46. Mason, S. F. *Quart. Rev. Chem. Soc. 17* (1963) 20.

Received February 25, 1986.